

Xth International school of neutron scattering Francesco Paolo Ricci

Detectors for neutron scattering

M. Tardocchi
tardocchi@ifp.cnr.it

Istituto di Fisica del Plasma, EURATOM-ENEA-CN
Association, Milan, Italy

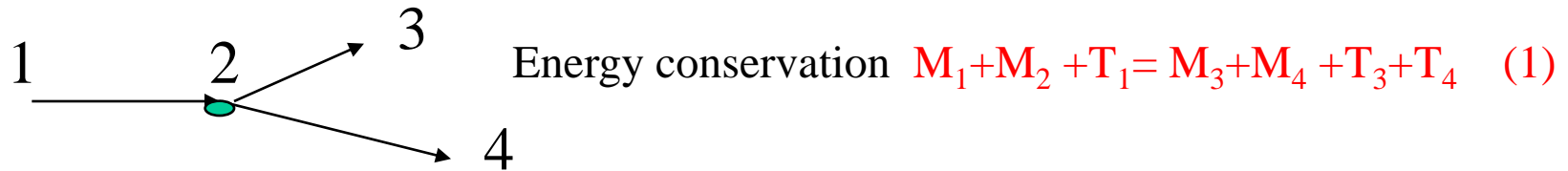
Nomenclature

Category	Energy [meV]	Temperature [K]	λ [Å]
Ultra-cold	< 0.1	< 1	< 30
Cold	0.1 – 10	1 – 120	30 – 3
Thermal	10– 25 -100	120 – 1000	3 – 1
Epithermal	> 500	> 6000	> 0.4
Fast	> ~ 10 ⁵	> 10 ⁶	>0.03

Neutron detection

- What does it mean detecting a neutron ?
 - Need to produce some sort of measurable quantitative (countable) electrical signal
 - It is not possible to detect directly slow neutrons (they carry too little energy). It can be done with fast neutrons
- Neutrons are non ionizing particles. They interact via nuclear force.
- Nuclear reactions needed to convert neutrons in charged secondary particles **(n, α)**, **(n,p)**, **(n, fission)**, **(n, γ)**
- Cross sections $\Sigma = N \cdot \sigma$; $\Sigma_{\text{tot}} = \Sigma_{\text{scatt}} + \Sigma_{\text{rad capt}} + \dots$; neutron flux Φ ($\text{n} \cdot \text{s}^{-1} \cdot \text{cm}^{-2}$)
- Typical charged particle detectors can be used:
 - Gaseous proportional counters & ionization chambers
 - Scintillation detectors
 - Semiconductors detectors
 - (n, γ) used in the Neutron Resonant Capture detector

Schematics of nuclear reactions



1 **Elastic collision** (rest) mass and T_{kin} are conserved; $M_1=M_2$; $M_3=M_4$

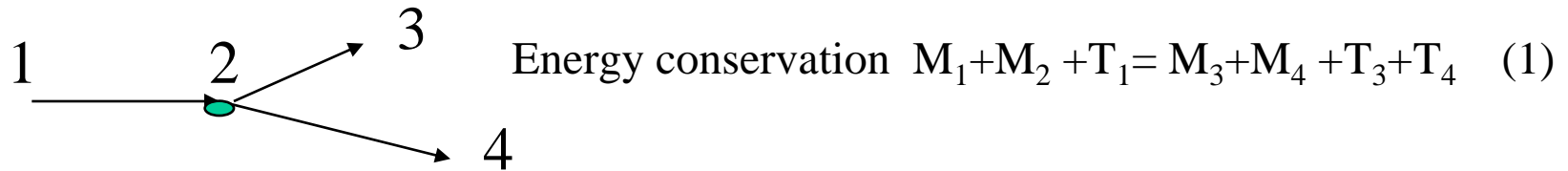
2 **Anelastic collision*** mass is conserved, T_{kin} is conserved

3 **Nuclear reactions** mass and T_{kin} are not conserved

$Q= (M_1+M_2) - (M_3+M_4)$ (2) Q-value definition

•Condensed matter scientist use the term **anelastic** to mean reaction of type 1 when $E_n \text{ initial} \neq E_n \text{ final}$ (exchange of $E = \hbar\omega$ and $Q = \hbar q$)

Schematics of nuclear reactions



eq1 +2 $(T_3 + T_4) - T_1 = Q$

$M_1 = M_3, M_2 = M_4$ and $Q = 0$

Elastic reactions

$M_1 = M_3, M_2 = M_4$ and $Q \neq 0$

Anelastic reactions

$Q < 0$ Endothermic Mass is created from kin. energy

$Q > 0$ Exothermic Mass is transformed in kinetic energy

$M_1 \neq M_3$ or $M_2 \neq M_4$ and $Q \neq 0$

Nuclear reactions ←

Some nuclear reactions for neutron detection

- $n + {}^3\text{He} \rightarrow {}^3\text{H} + {}^1\text{H} + 0.764 \text{ MeV}$
- $n + {}^6\text{Li} \rightarrow {}^4\text{He} + {}^3\text{H} + 4.79 \text{ MeV}$
- $n + {}^{10}\text{B} \rightarrow {}^7\text{Li}^* + {}^4\text{He} \rightarrow {}^7\text{Li} + {}^4\text{He} + 0.48 \text{ MeV } \gamma + 2.3 \text{ MeV (93\%)}$
 $\qquad\qquad\qquad \rightarrow {}^7\text{Li} + {}^4\text{He} \qquad\qquad\qquad + 2.8 \text{ MeV (7\%)}$
- $n + {}^{155}\text{Gd} \rightarrow \text{Gd}^* \rightarrow \gamma\text{-ray spectrum} \rightarrow \text{conversion electron spectrum}$
- $n + {}^{157}\text{Gd} \rightarrow \text{Gd}^* \rightarrow \gamma\text{-ray spectrum} \rightarrow \text{conversion electron spectrum}$
- $n + {}^{235}\text{U} \rightarrow \text{fission fragments} + \sim 160 \text{ MeV}$
- $n + {}^{239}\text{Pu} \rightarrow \text{fission fragments} + \sim 160 \text{ MeV}$

Detectors for slow neutrons

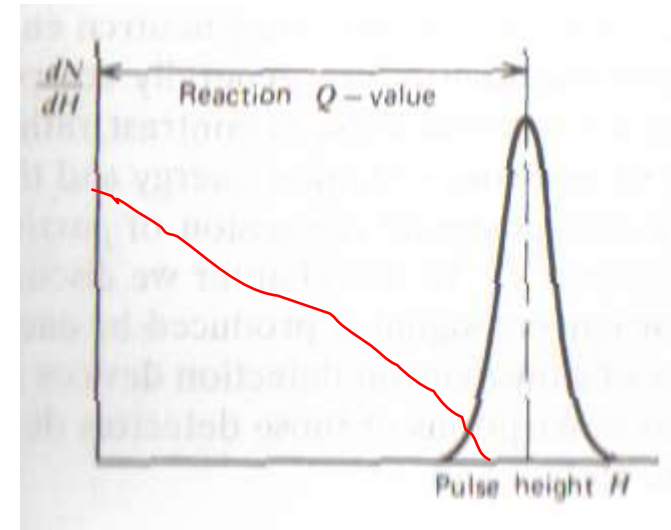
Ideal detector:

High detection efficiency (cross section)

Large Q values

Stop reaction products

Immune to background (often γ rays)



E_{kinetics} of the products = $Q + \cancel{E_n} = Q$

Products emitted back-to-back ($P_{\text{init}} \sim 0$)

$$\begin{cases} E_3 + E_4 = Q \\ m_3 v_3 + m_4 v_4 = 0 \end{cases} \quad \dots \quad E_{3,4} = \frac{m_{4,3}}{m_3 + m_4} \cdot Q$$

Reactions for slow neutron detection

- $n + {}^{10}\text{B}$ (a.i.20%) $\rightarrow {}^7\text{Li}^* + \alpha \rightarrow {}^7\text{Li} + \alpha + 0.48 \text{ MeV } \gamma + 2.3 \text{ MeV}$ (93%) 3840 barns
 $\rightarrow {}^7\text{Li} + {}^4\text{He} + 2.8 \text{ MeV}$ (7%)
- $n + {}^3\text{He} \rightarrow {}^3\text{H} + {}^1\text{H} + 0.764 \text{ MeV}$ (expensive) **5330 barns**
- $n + {}^6\text{Li}$ (a.i. 7%) $\rightarrow {}^4\text{He} + {}^3\text{H} + 4.79 \text{ MeV}$ (resonance at 100keV) 940 barns

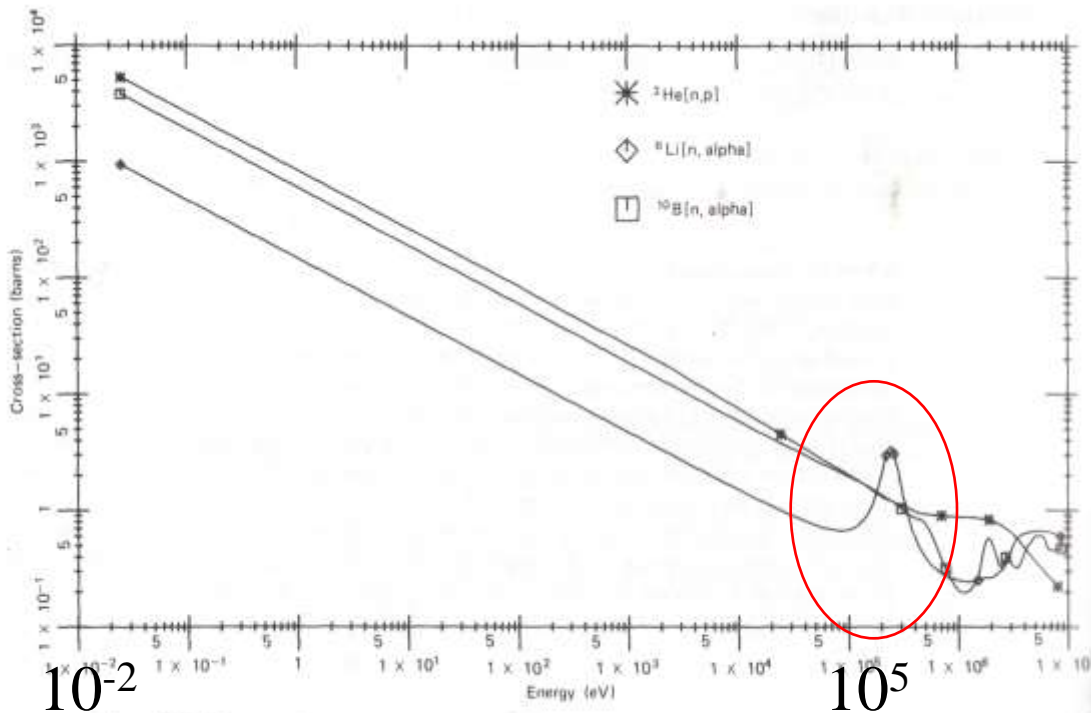


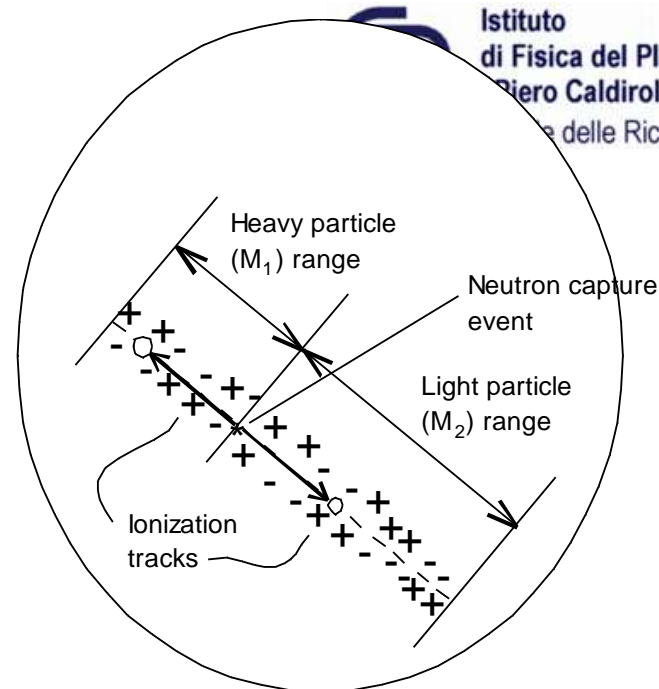
Figure 14.1 Cross section versus neutron energy for some reactions of interest in neutron detection.

Gas Detectors

Ionization tracks in
proportional counter gas

Neutron
→

Electrons drift toward the central anode wire. When they get close, they accelerate sufficiently between collisions with gas atoms to ionize the next atom. A *Townsend avalanche* occurs in which the number of electrons (and ions) increases the number many-fold, about $\times 10^3$. Separation of these charges puts a charge on the detector, which is a low-capacitance capacitor, causing a pulse in the voltage that can be amplified and registered electronically.



Gas Detectors – operational modes

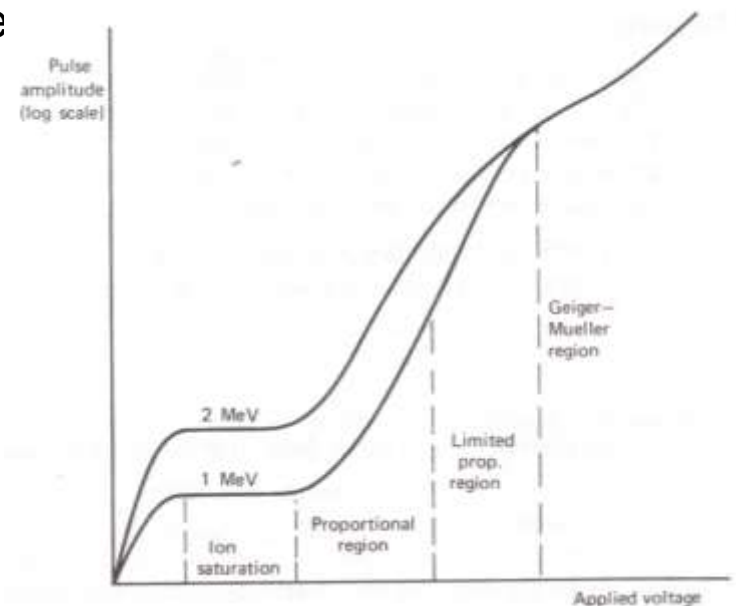
Ionization Mode

Electrons drift to anode, producing a charge pulse with no gas multiplication. Typically employed in low-efficiency beam-monitor detectors.

Proportional Mode: electron collisions ionize gas atoms producing even more electrons.

Gas amplification increases the collected charge proportional to the initial charge produced.

Gas gains of up to a few thousand are possible, above which proportionality is lost.



Proportional counters (PCs) come in a variety of different forms.

Simple detector

Linear position-sensitive detector (LPSD):

The anode is resistive, read out from both ends—the chargedistributes between the ends according to the position of the neutron capture event in the tube.

Usually cylindrical.

2-D position-sensitive detector (MWPC).

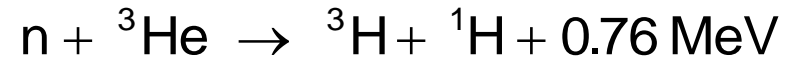
Many parallel resistive wires extend across a large thick area of fill gas. Each wire operates either as in LPSD or without position. information as in a simple PC.

or

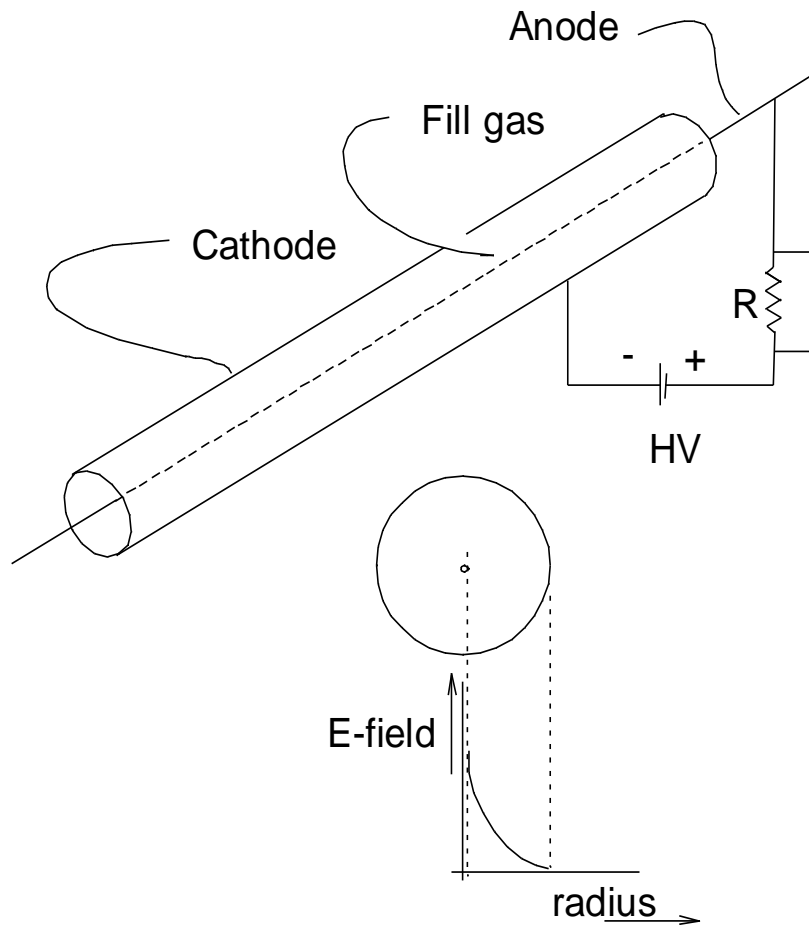
Two mutually perpendicular arrays of anode wires. Each is read separately as an LPSD to give two coordinates for the neutron capture event.

MWPCs usually have a planar configuration.

Gas proportional counter

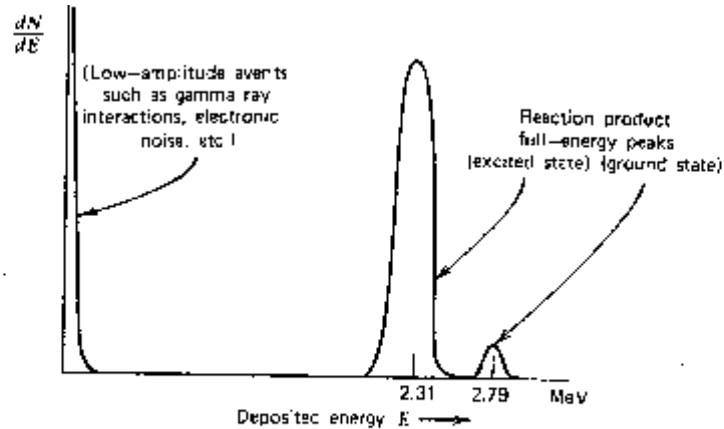


$$\sigma = 5333 \frac{\lambda}{1.8} \text{ barns}$$

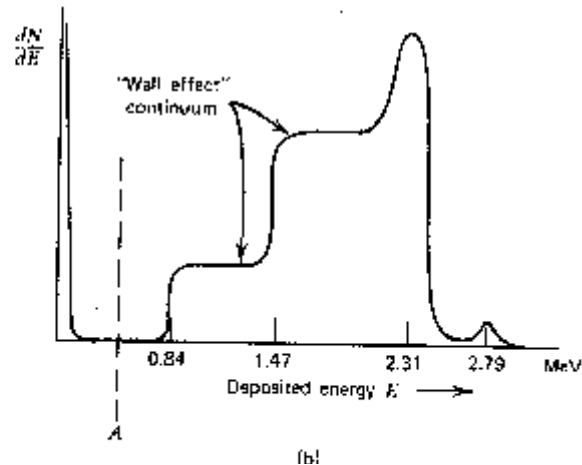


~25,000 ions and electrons
produced per neutron

BF₃ detector response function



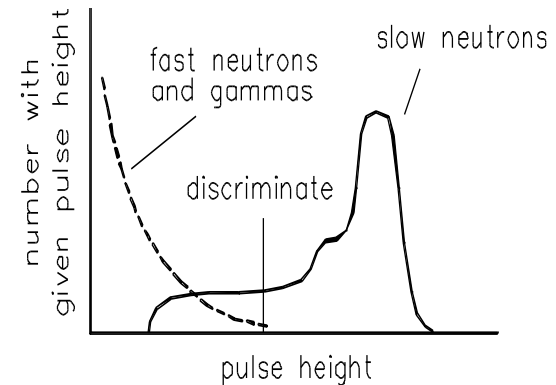
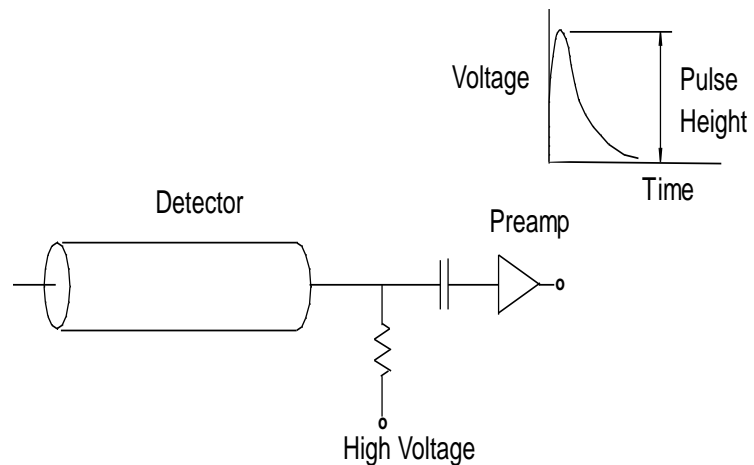
For large BF₃ detectors the secondaries are completely absorbed



In small BF₃ wall effect is present

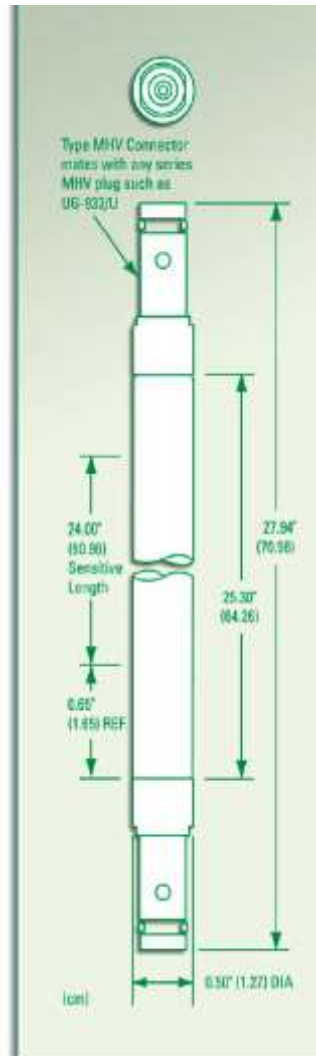
Range in BF₃ $\alpha \sim 1 \text{ cm @ 1 ATM}$

Pulse Height Discrimination

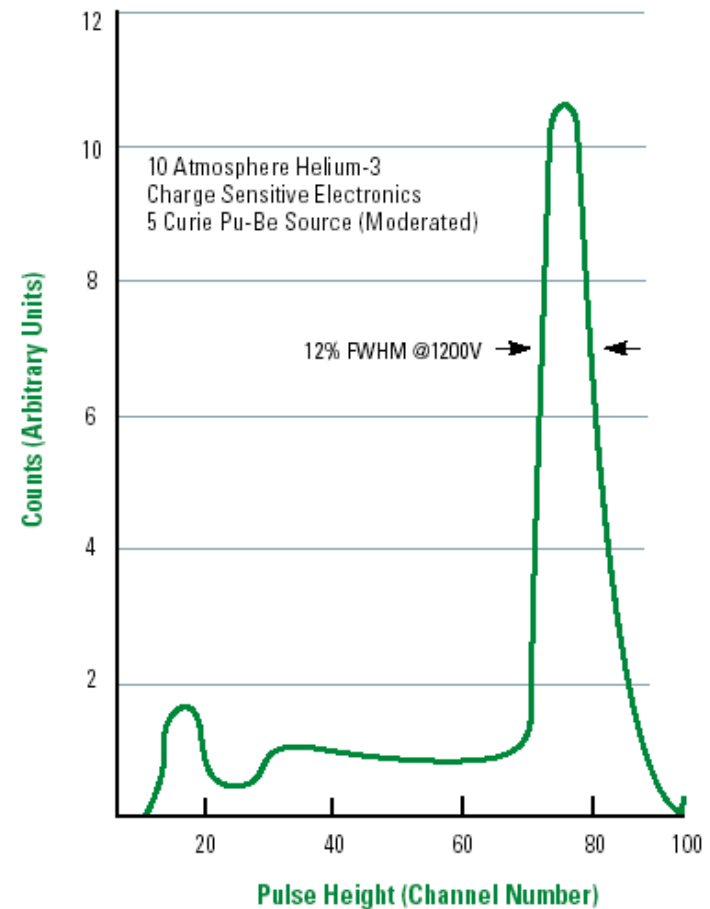


- Can set discriminator levels to reject undesired events (fast neutrons, gammas, electronic noise).
- Pulse-height discrimination can make a large improvement in background.
- Discrimination capabilities are an important criterion in the choice of detectors (^3He gas detectors are very good).

Reuter-Stokes LPSD



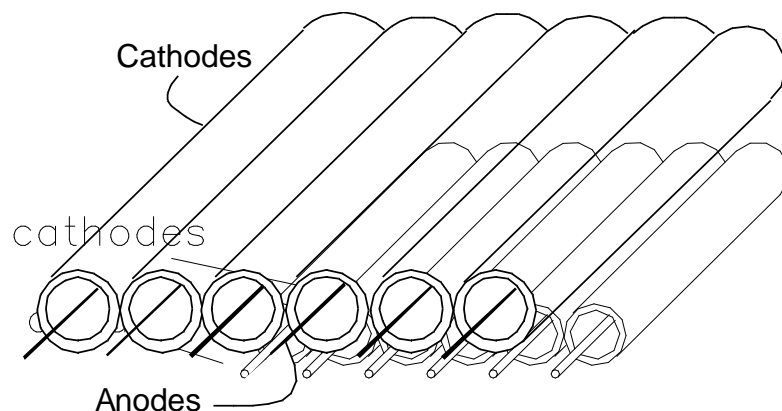
Typical Differential Pulse Height Spectrum



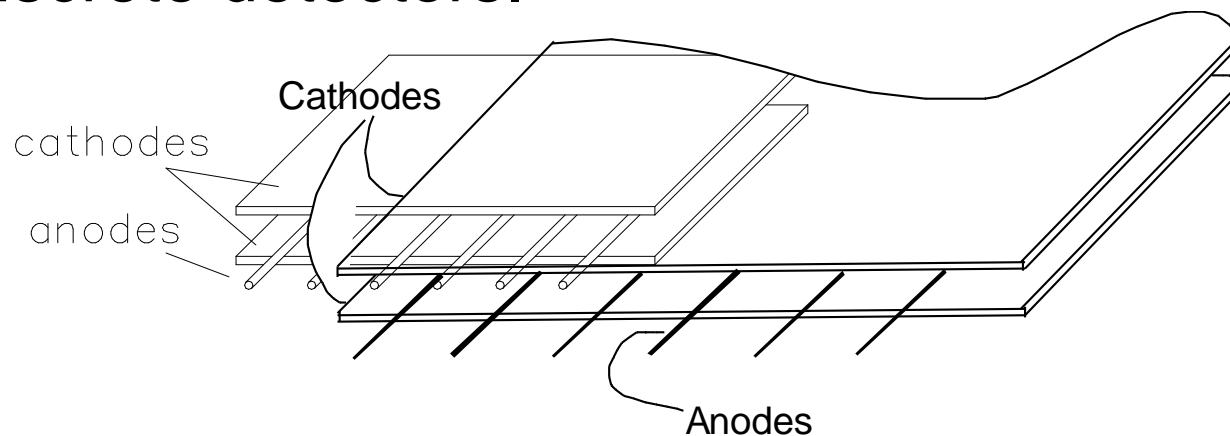
MAPS LPSD Detector Bank (at ISIS)



Multi-Wire Proportional Counter

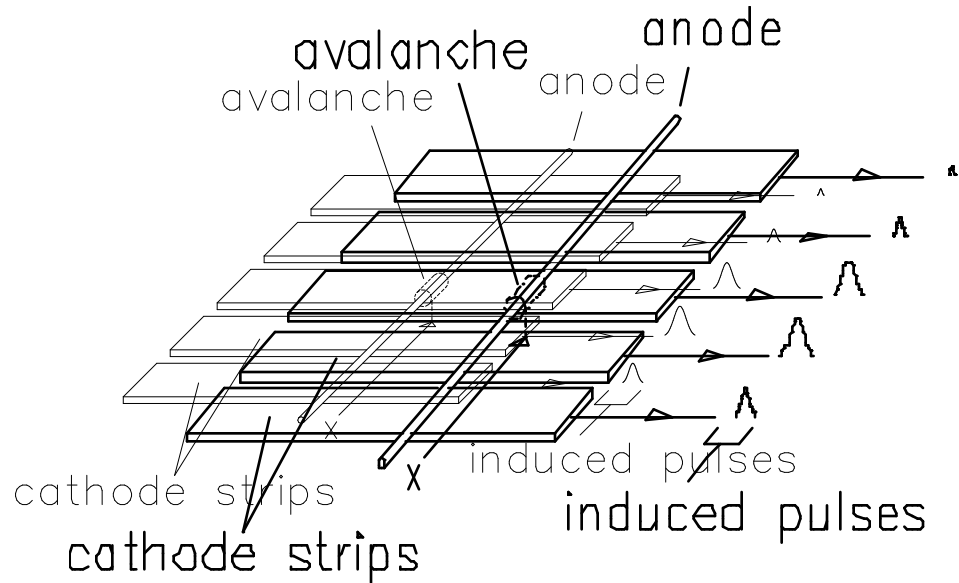


- Array of discrete detectors.



- Remove walls to get multi-wire counter.

MWPC

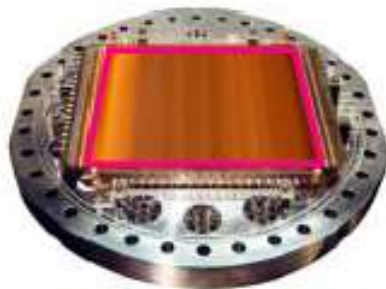


- Segment the cathode to get x-y position

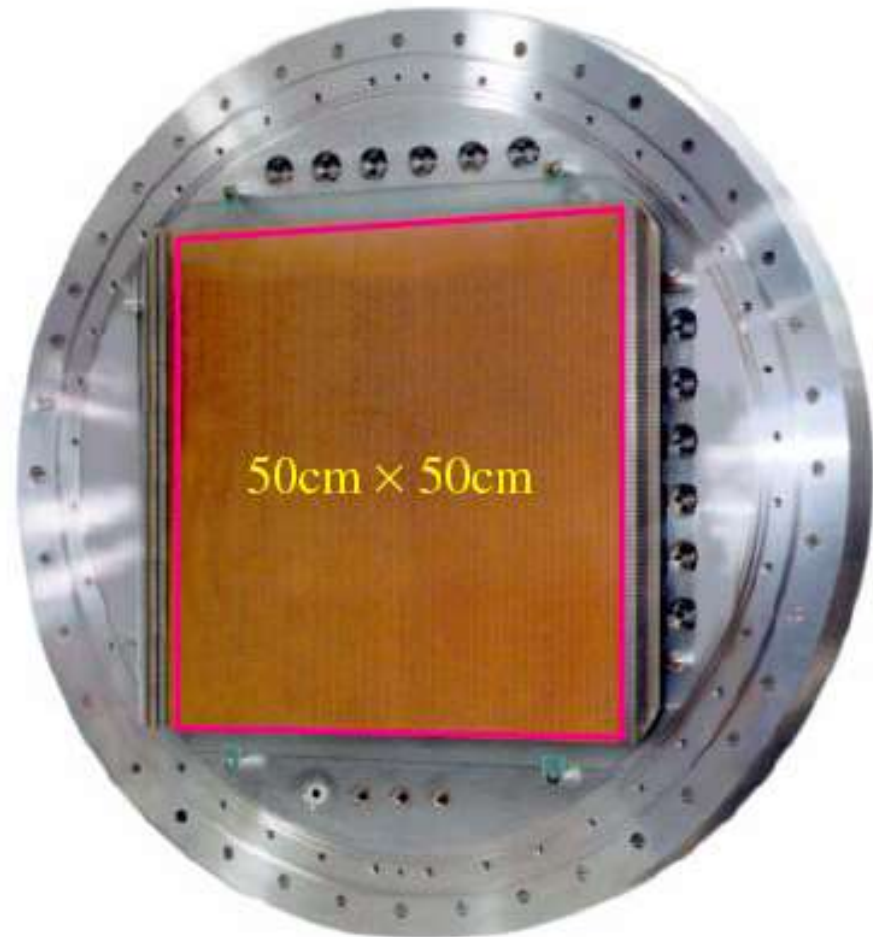
Brookhaven MWPCs



5cm × 5cm



20cm × 20cm



50cm × 50cm

Efficiency of Detectors

Detectors rarely register all the incident neutrons. The ratio of the number registered to the number incident is the efficiency.

- Full expression: $eff = 1 - \exp(-N \cdot \sigma \cdot d)$.

- Approximate expression for low efficiency:

$$eff = N \cdot \sigma \cdot d.$$

- Here:

σ = absorption cross-section (function of wavelength)

N = number density of absorber

d = thickness

$N = 2.7 \times 10^{19} \text{ cm}^{-3}$ per atm for a gas at 300 K.

For 1-cm thick ^3He at 1 atm and 1.8-Å neutrons, $\varepsilon = \mathbf{0.13}$.

For a real 3d detector geometry Monte Carlo codes are needed in order to calculate the detector efficiency,

Spatial resolution (how well the detector tells the location of an event) is always limited by the charged-particle range and by the range of neutrons in the fill gas, which depend on the pressure and composition of the fill gas.

And by the geometry:

Simple PCs: $\delta z \sim \text{diameter}$; 6 mm - 50 mm.

LPSDs: $\delta z \sim \text{diameter}$, $\delta y \sim \text{diameter}$; 6 mm - 50 mm.

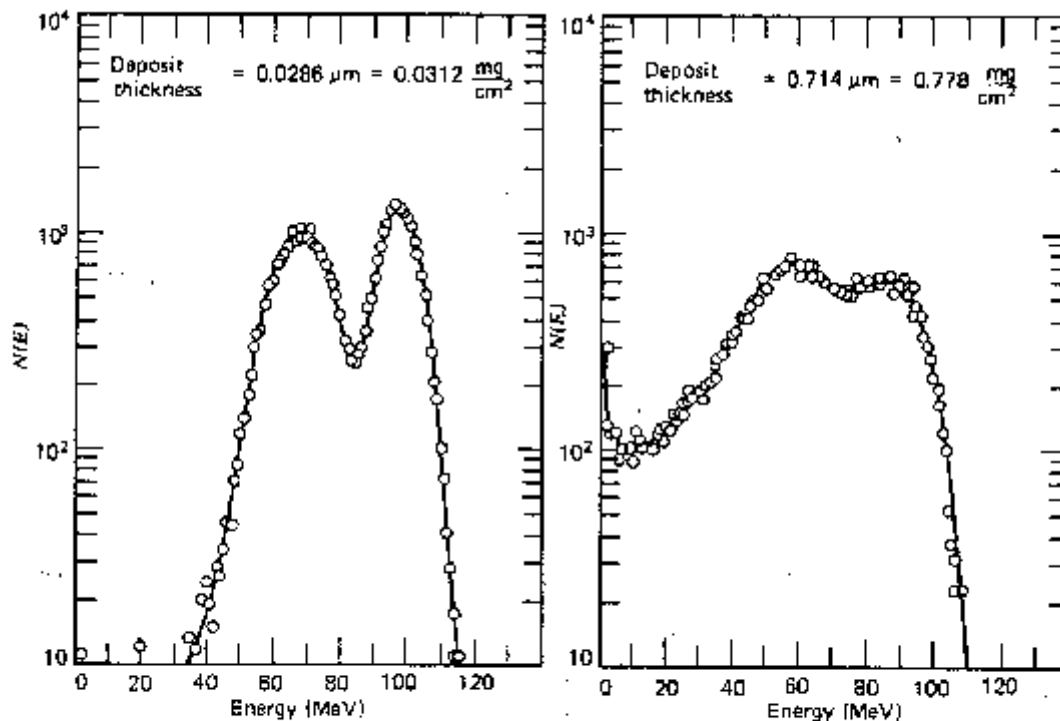
MWPC: δz and $\delta y \sim \text{wire spacing}$; 1 mm - 10 mm.

Fission Counters

Ionization chamber coated in its inner surface with fissile deposit.

One of the the two fission fragment can be detected.

Very large Q value (180-200MeV)

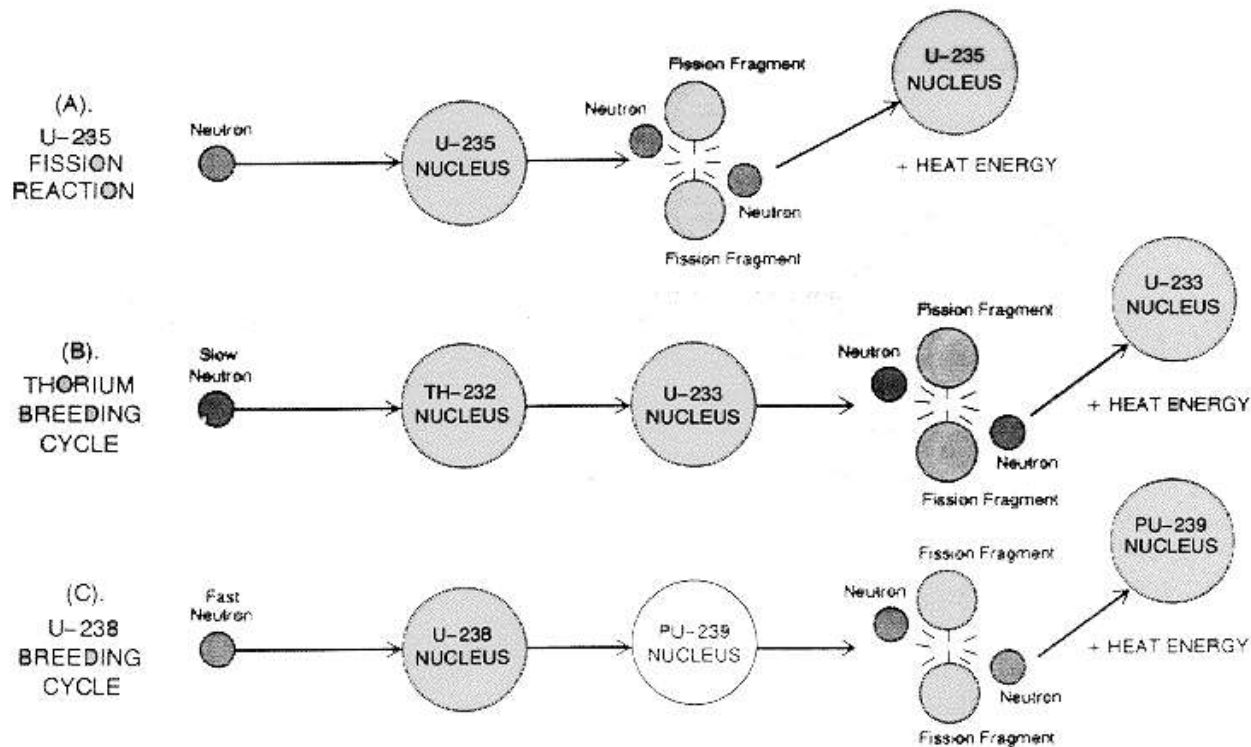


With large thickness of fissile material deposition (UO_2) the fission fragments may lose a significant fraction of their energy in the material itself thus releasing less energy into the detector

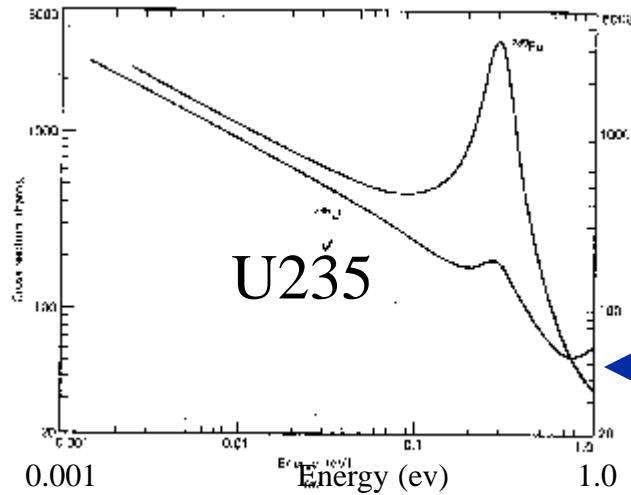
Figure 14.7 Energy spectra of fission fragments emerging from flat UO_2 deposits of two different thicknesses. A 2π detector is assumed which responds to fragments emitted in all directions from one surface of the deposit. (From Kahn et al.²⁶)

The fission reaction

FIGURE 1: Three nuclear reactions: one using naturally fissile U_{235} and two which breed fissile materials from U_{238} and Th_{232} .



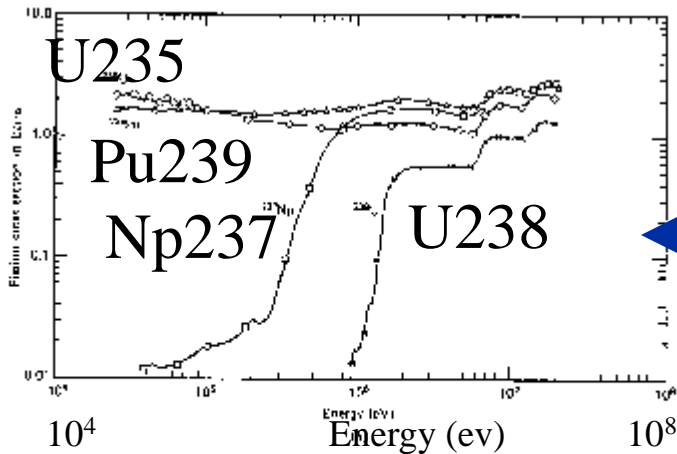
Fission cross sections



Pu239

U235

Thermal neutron region



U235

Pu239

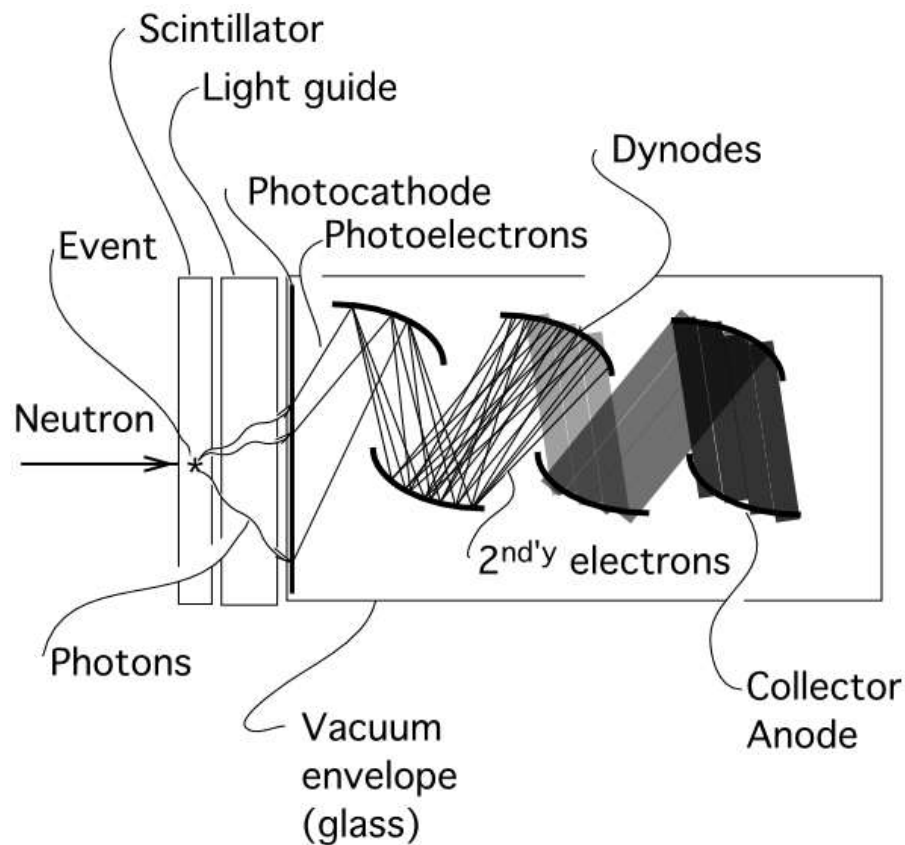
Np237

U238

Fast neutron region

Figure 14.2 Fast fission cross sections of some common target nuclides used in fission chambers. (a) Slow neutron region, where the cross sections shown are relatively large. (b) Fast neutron region. Chambers with ^{237}Np or ^{238}U are used as threshold detectors sensitive only to fast neutrons.

Scintillation Detectors



$$\sigma = 940 \frac{\lambda}{1.8} \text{ barns}$$

Some Common Scintillators for Neutron Detectors

Intrinsic scintillators contain small concentrations of ions (“wave shifters”) that shift the wavelength of the originally emitted light to the longer wavelength region easily sensed by photomultipliers.

ZnS(Ag) is the brightest scintillator known, an intrinsic scintillator that is mixed heterogeneously with converter material, usually Li^6F in the “Stedman” recipe, to form scintillating composites. These are only semitransparent. But it is somewhat slow, decaying with $\sim 10 \mu\text{sec}$ halftime.

GS-20 (glass, Ce^{3+}) is mixed with a high concentration of Li_2O in the melt to form a material transparent to light.

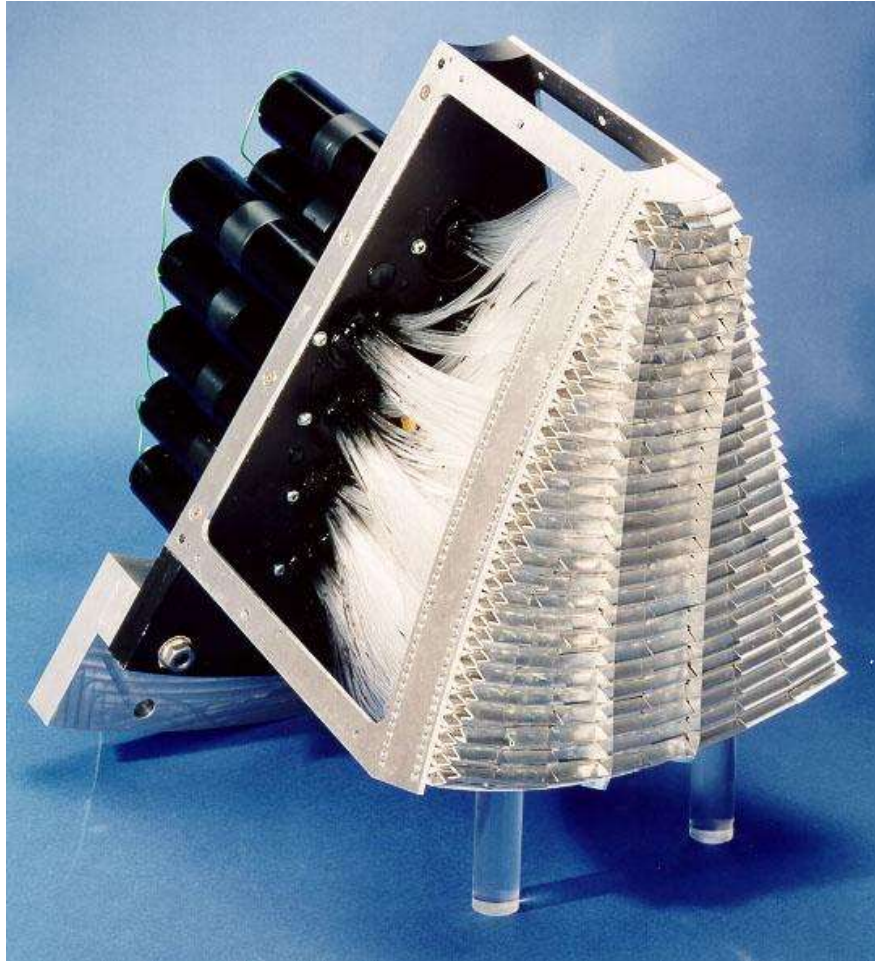
$\text{Li}_6\text{Gd}(\text{BO}_3)_3 (\text{Ce}^{3+})$ (including ^{158}Gd and ^{160}Gd , ^6Li , and ^{11}B), and $^6\text{LiF}(\text{Eu})$ are intrinsic scintillators that contain high proportions of converter material and are typically transparent.

An efficient gamma ray detector with little sensitivity to neutrons, used in conjunction with neutron capture gamma-ray converters, is **YAP** (yttrium aluminum perovskite, $\text{YAl}_2\text{O}_3(\text{Ce}^{3+})$).

Some Common Scintillators for Neutron Detectors

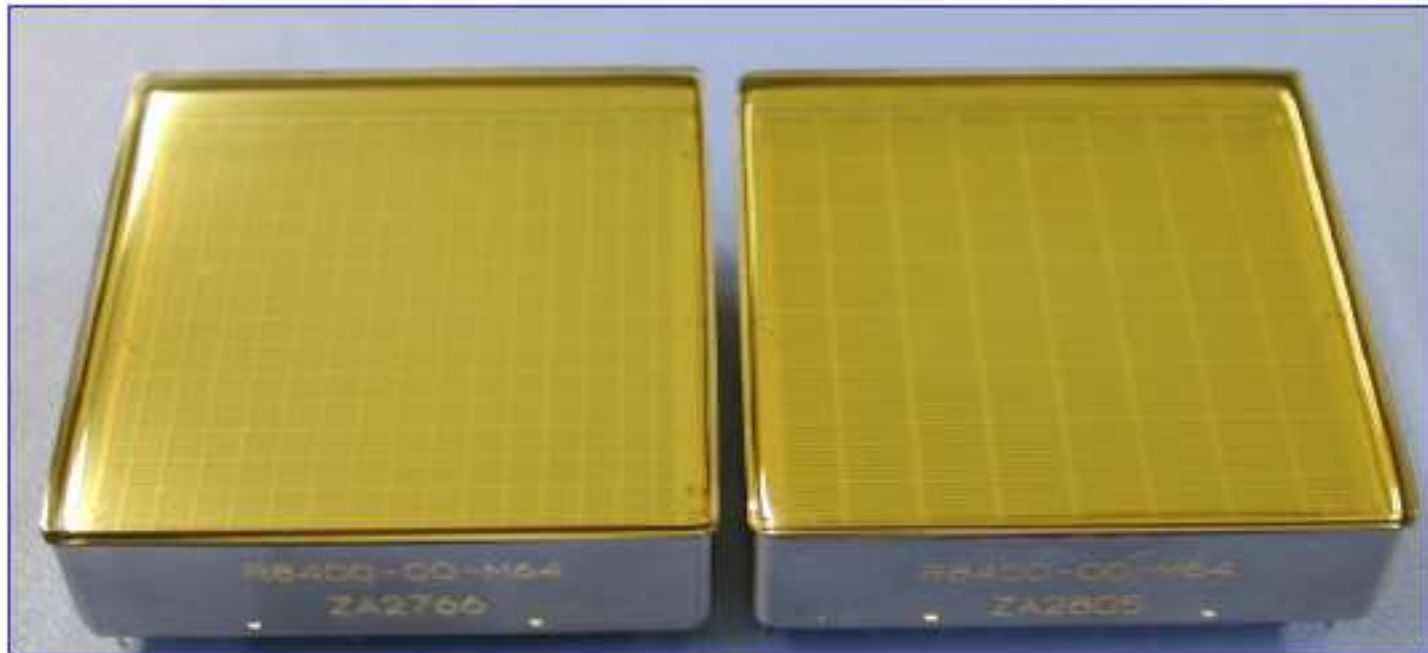
Material	Density of ${}^6\text{Li}$ atoms (cm^{-3})	Scintillation efficiency	Photon wavelength (nm)	Photons per neutron
Li glass (Ce)	1.75×10^{22}	0.45 %	395 nm	~7,000
LiI (Eu)	1.83×10^{22}	2.8 %	470	~51,000
ZnS (Ag) - LiF	1.18×10^{22}	9.2 %	450	~160,000
$\text{Li}_6\text{Gd}(\text{BO}_3)_3$ (Ce),	3.3×10^{22}		~ 400	~40,000
YAP	--		350	~18,000 per MeV gamma

GEM Detector Module (at ISIS)



Hamamatsu Multicathode Photomultiplier

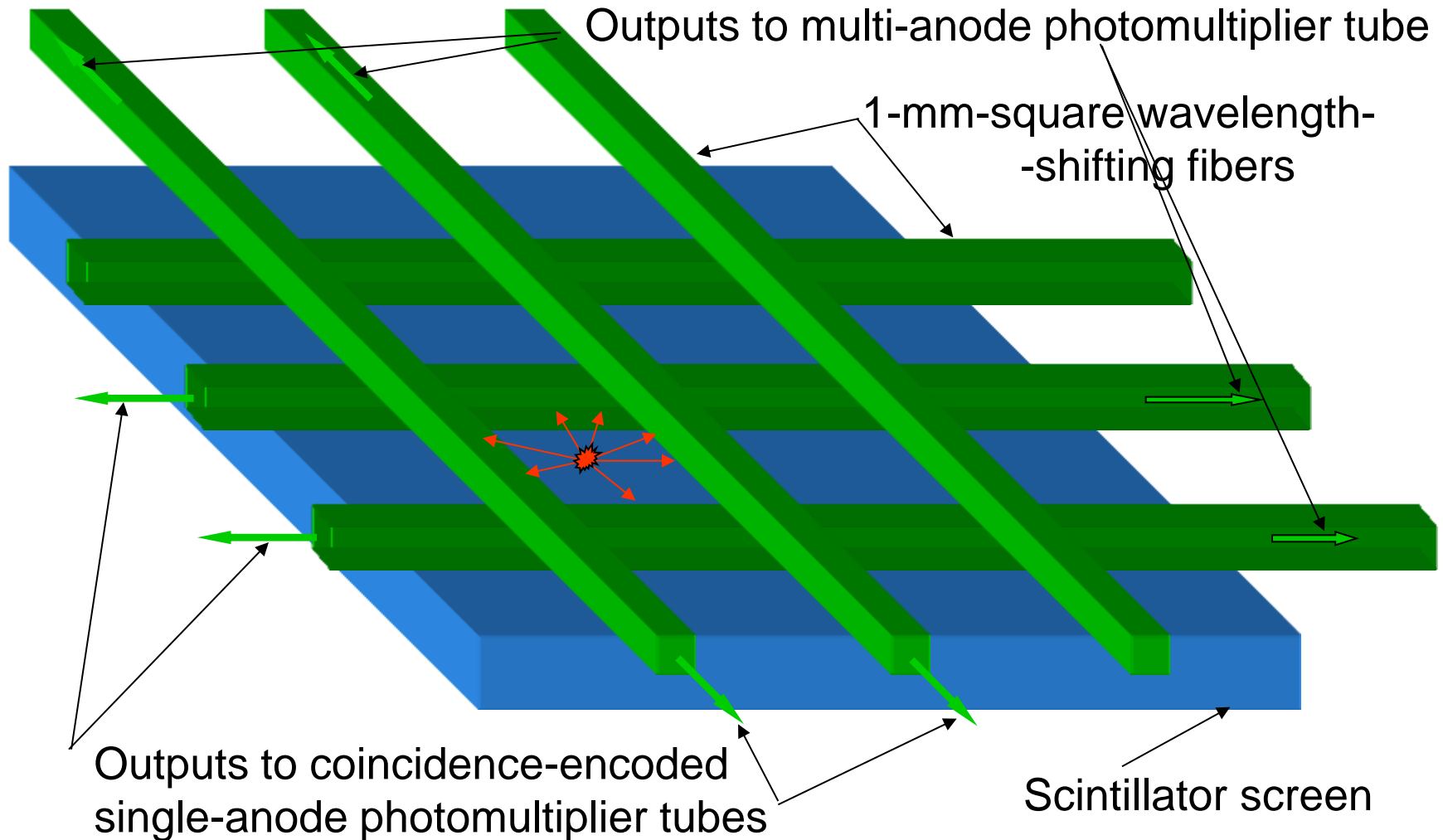
Compact photomultipliers are essential components of scintillation area detectors. The figure shows a recently developed multicathode photomultiplier, Hamamatsu model 8500.



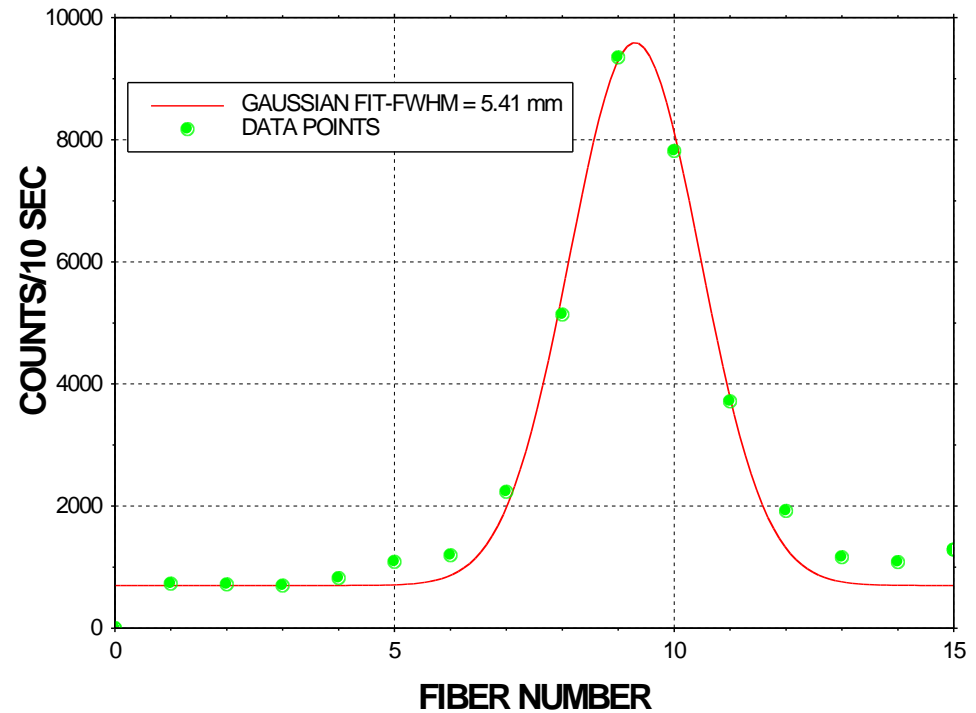
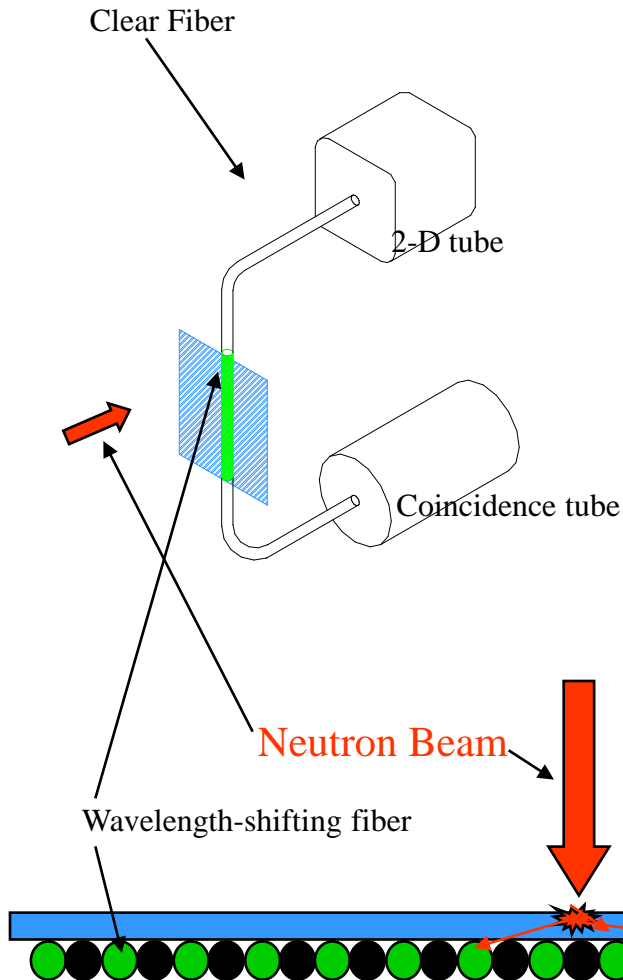
256 ch Focusing Type

64 ch Focusing Type

Principle of Crossed-Fiber Position-Sensitive Scintillation Detector



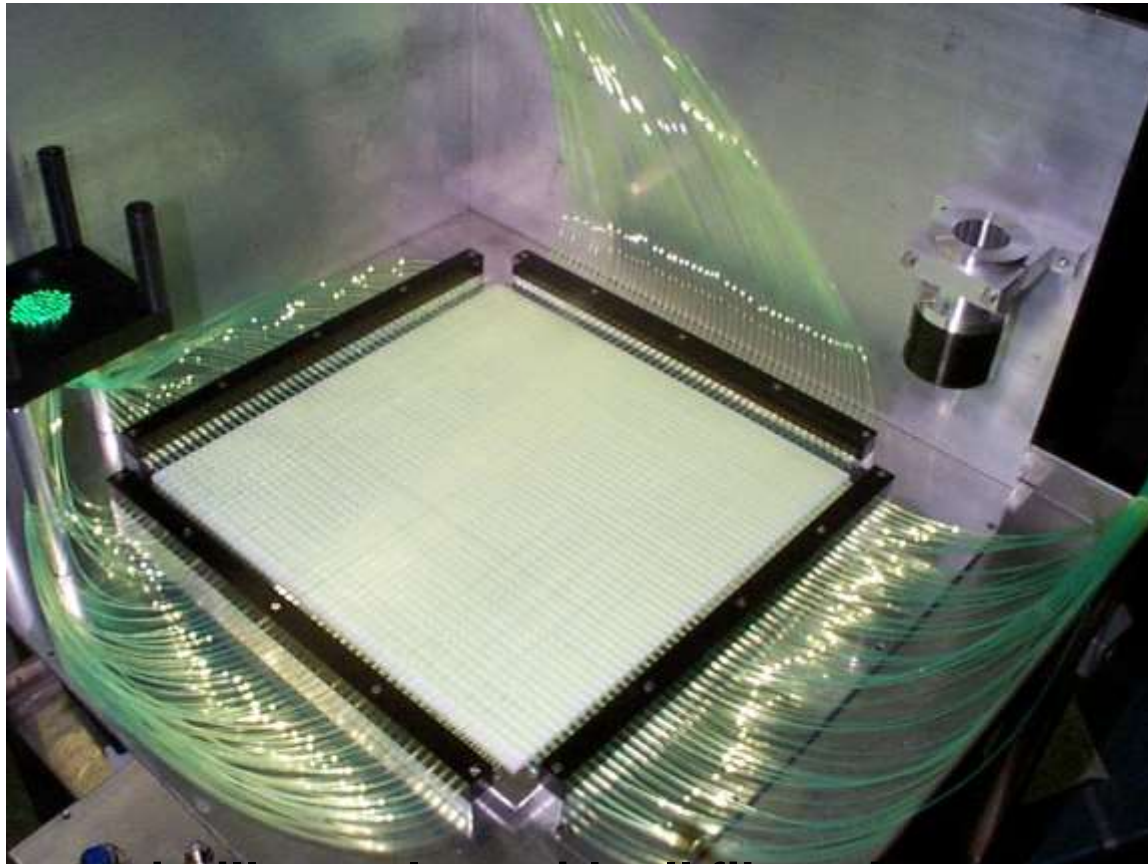
16-element WAND Prototype Schematic and Results



Crossed-Fiber Scintillation Detector Design Parameters (ORNL I&C)

- Size: 25-cm x 25-cm.
- Thickness: 2-mm.
- Number of fibers: 48 for each axis.
- Multi-anode photomultiplier tube: Phillips XP1704.
- Coincidence tube: Hamamastu 1924.
- Resolution: < 5 mm.
- Shaping time: 300 nsec.
- Counting-rate capability: ~ 1 MHz.
- Time-of-flight resolution: 1 μ sec.

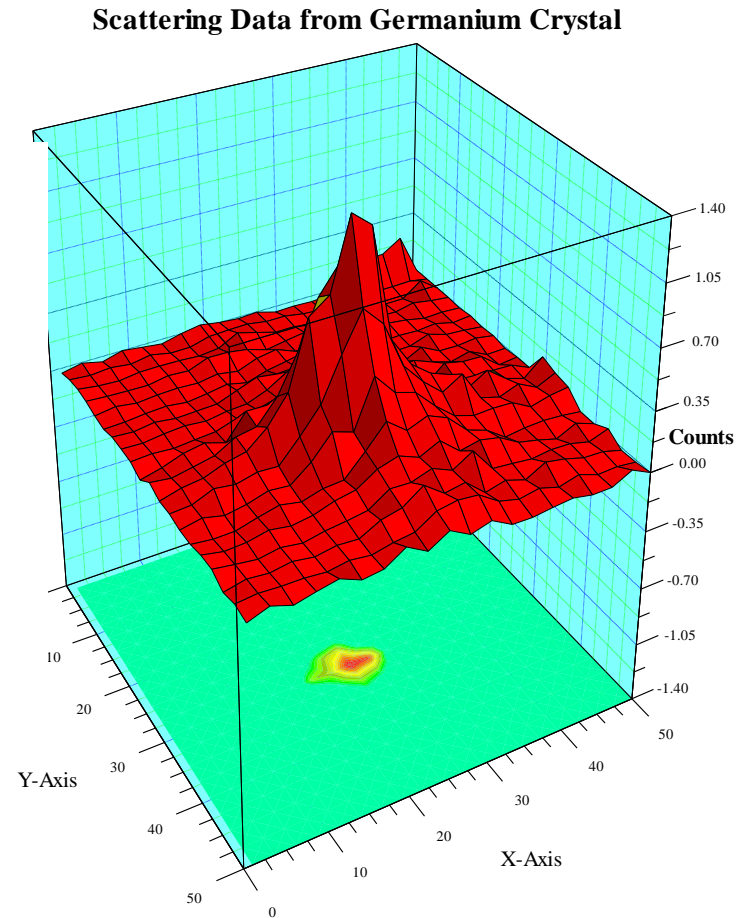
SNS 2-D Scintillation Detector Module



Shows scintillator plate with all fibers installed and connected to multi-anode photomultiplier mount.

Neutron Scattering from Germanium Crystal Using Crossed-Fiber Detector

- Normalized scattering from 1-cm-high germanium crystal.
- $E_n \sim 0.056$ eV.
- Detector 50 cm from crystal.



Neutron Detector Screen Design

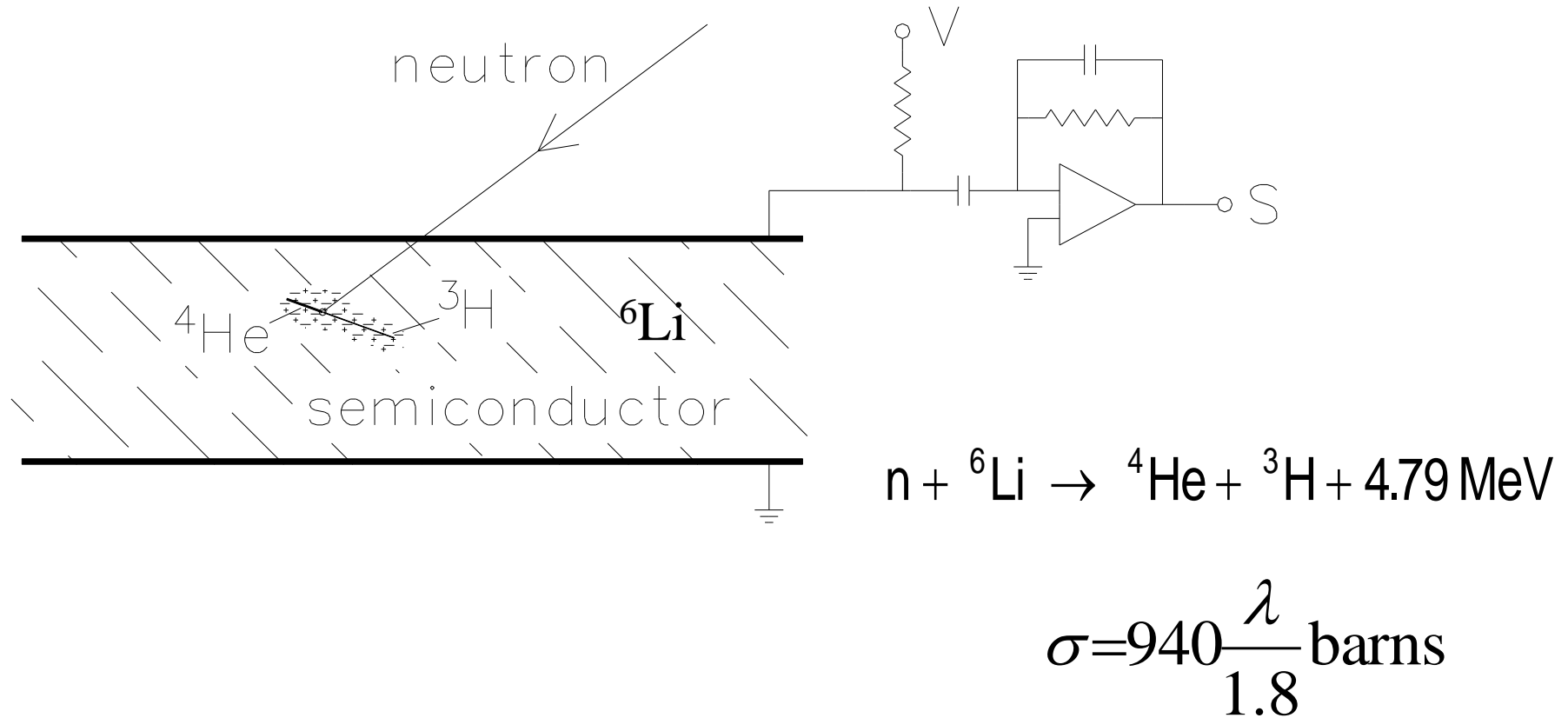
The scintillator screen for this 2-D detector consists of a mixture of ${}^6\text{LiF}$ and silver-activated ZnS powder in an optical grade epoxy binder. Neutrons incident on the screen react with the ${}^6\text{Li}$ to produce a triton and an alpha particle. These charged particles passing through the ZnS(Ag) cause it to emit light at a wavelength of approximately 450 nm. The 450-nm photons are absorbed in the wavelength-shifting fibers where they convert to 520-nm photons, some of which travel toward the ends of the fibers guided by critical internal reflection. The optimum mass ratio of ${}^6\text{LiF}:\text{ZnS}(\text{Ag})$ is about 1:3.

The screen is made by mixing the powders with uncured epoxy and pouring the mix into a mold. The powder settles to the bottom of the mold before the binder cures. The clear epoxy above the settled powder mix is machined away. The mixture of 40 mg/cm² of ${}^6\text{LiF}$ and 120 mg/cm² of ZnS(Ag) used in this screen provides a measured neutron conversion efficiency of over 90% for 1.8 Å neutrons.

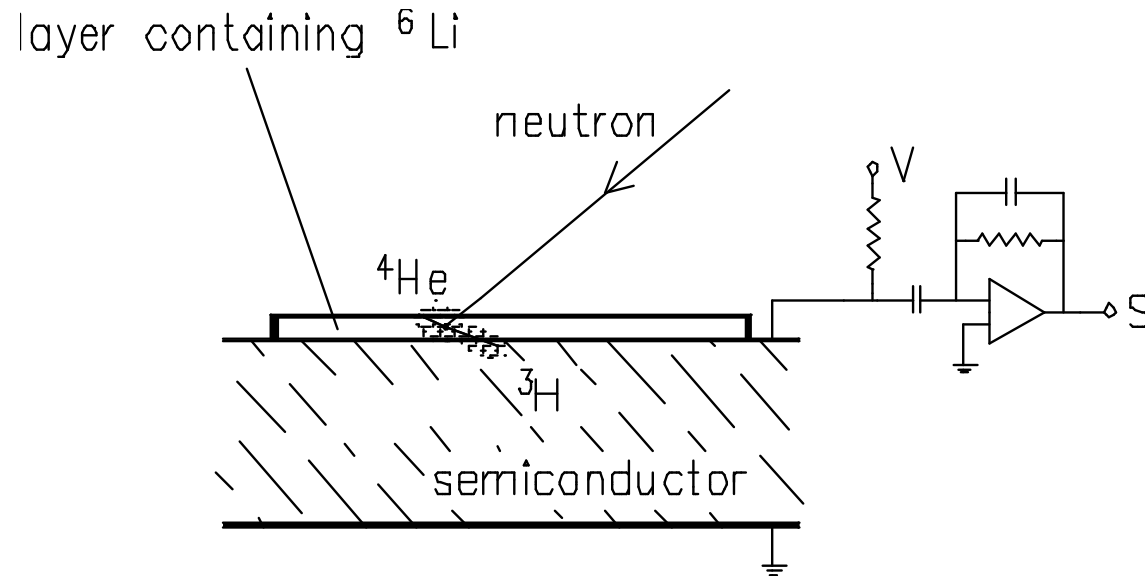
The spatial resolution accomplishable in SDs is typically better than in gas detectors. The range of neutrons is less. The range of ionizing particles is less in solid materials than in gases.

However, the localization of the light source (an optical process) imposes the limit on position resolution. This in turn depends statistically on the number of photons produced in the scintillator (more is better, of course).

Semiconductors detectors



Coating with Neutron Absorber-Surface-Barrier Detectors



- Layer (${}^6\text{Li}$ or ${}^{10}\text{B}$) must be thin (a few microns) for charged particles to reach the detector.
 - Detection efficiency is low.
- Most of the deposited energy doesn't reach detector.
 - Poor pulse-height discrimination

Semiconductor Detectors

$\sim 1.5 \times 10^6$ holes and electrons produced per neutron
(large number compared to scintillator and gas detectors)

The detector acts as a capacitor. The ionization partially discharges the capacitor and can be detected directly without further amplification.

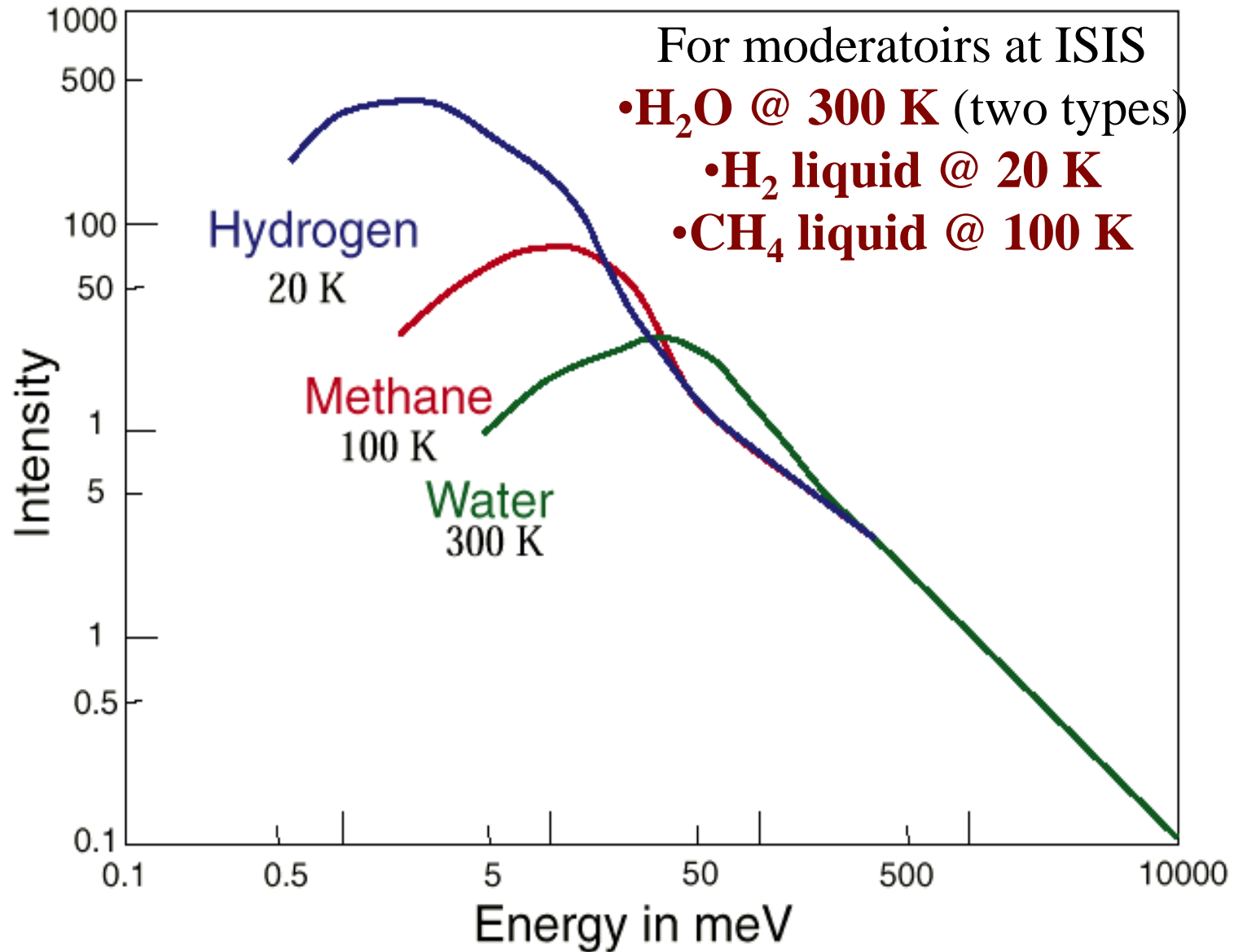
– However, standard device semiconductors do not contain enough neutron-absorbing nuclei to give reasonable **neutron detection efficiency**. Options:

i) *Put neutron absorber on surface of semiconductor?*

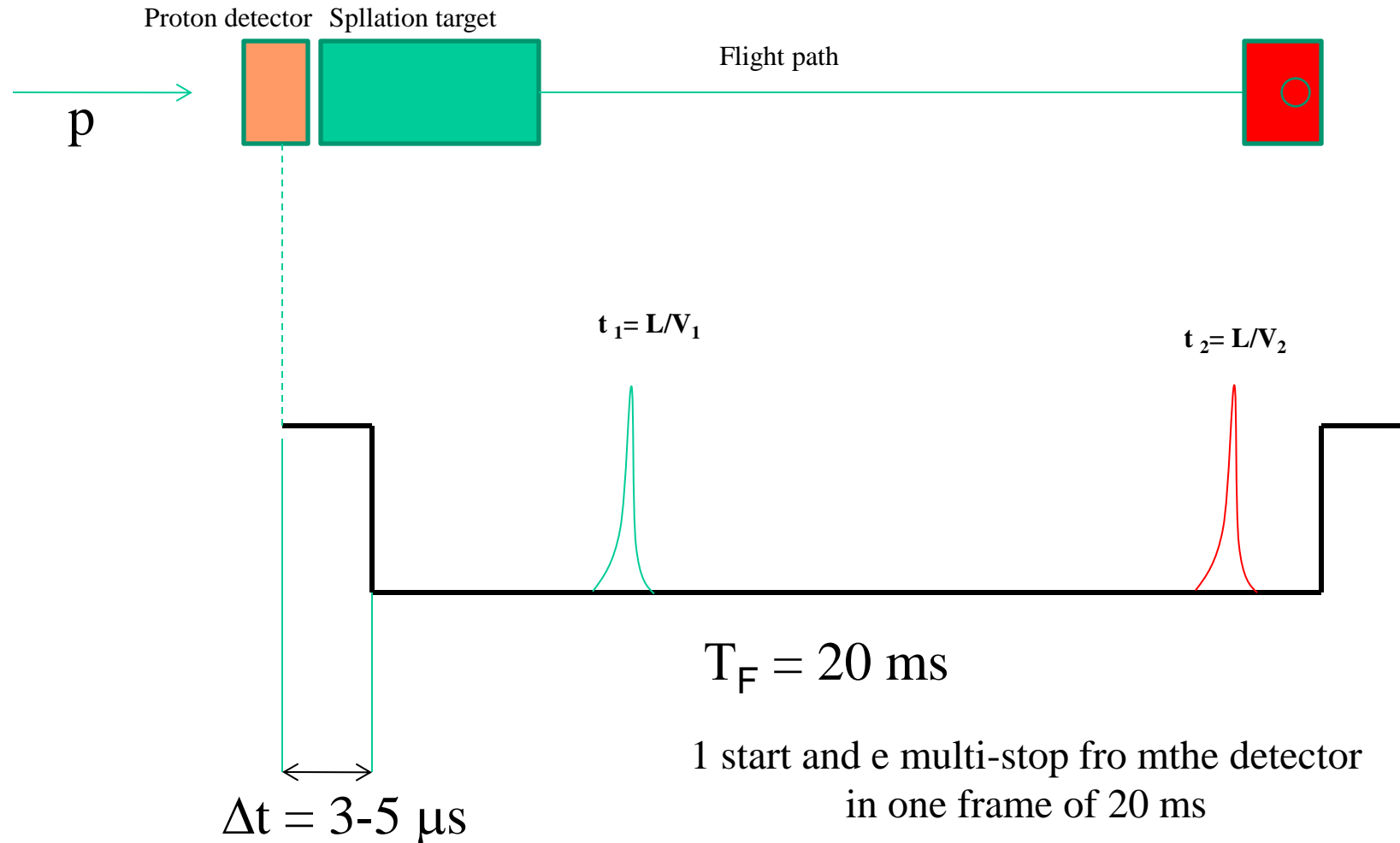
These exist and are called surface barrier detectors.

ii) *Develop, for example, boron phosphide semiconductor devices? This is a challenge for future development.*

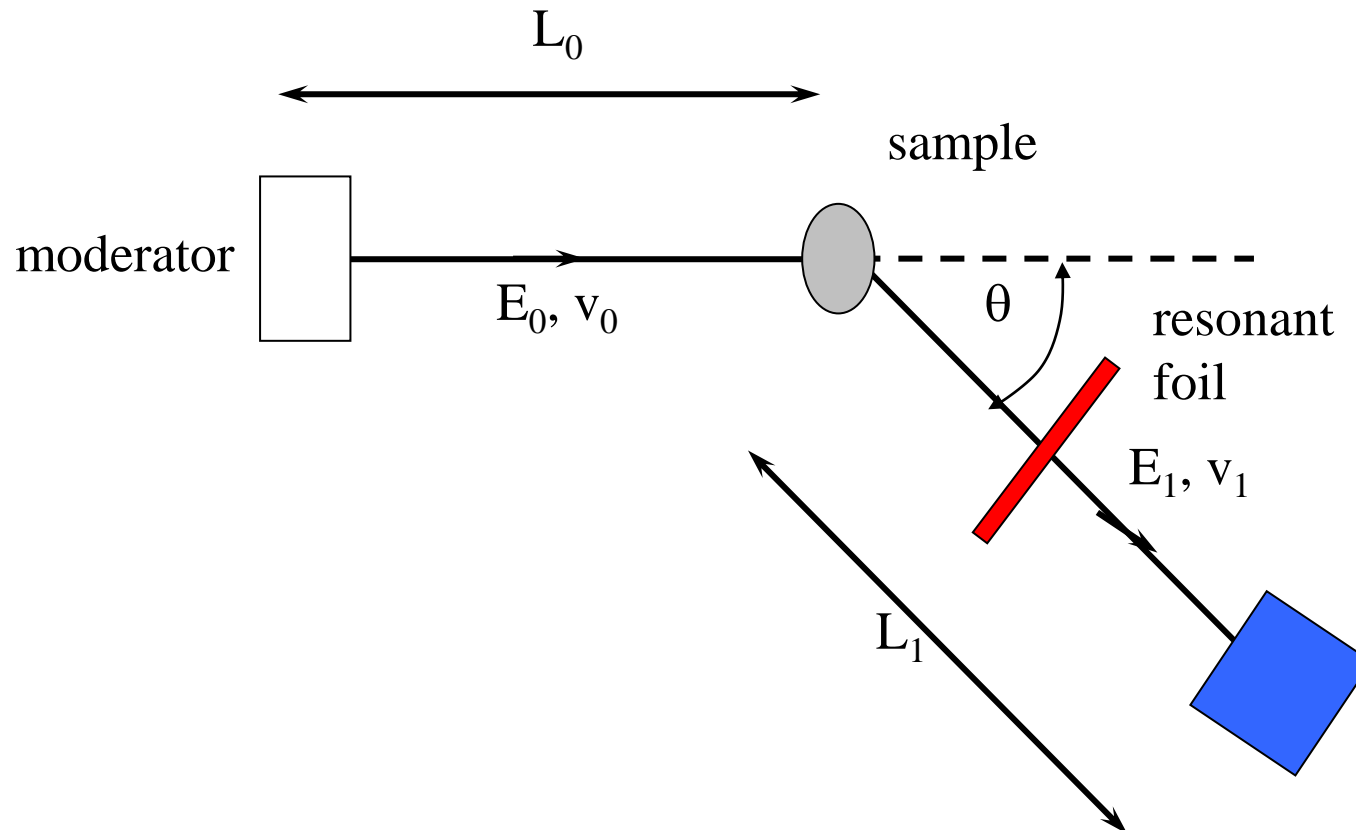
Epithermal neutrons from spallation sources



The Time of flight technique



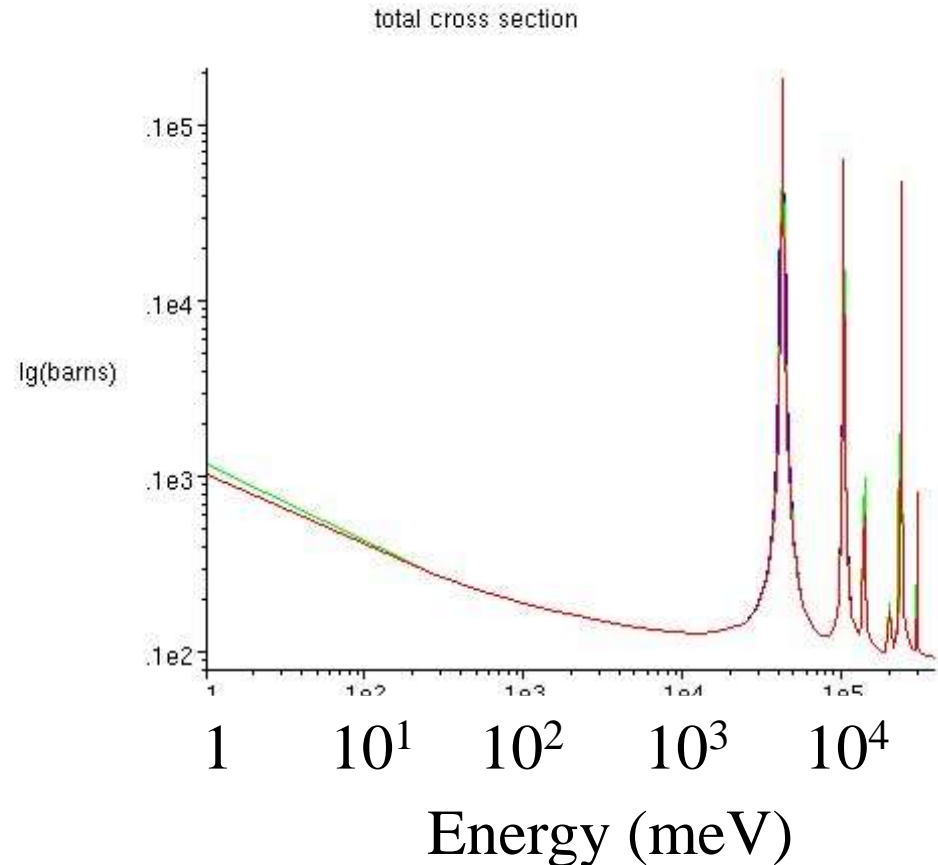
Time of flight neutron spectroscopy in inverted geometry



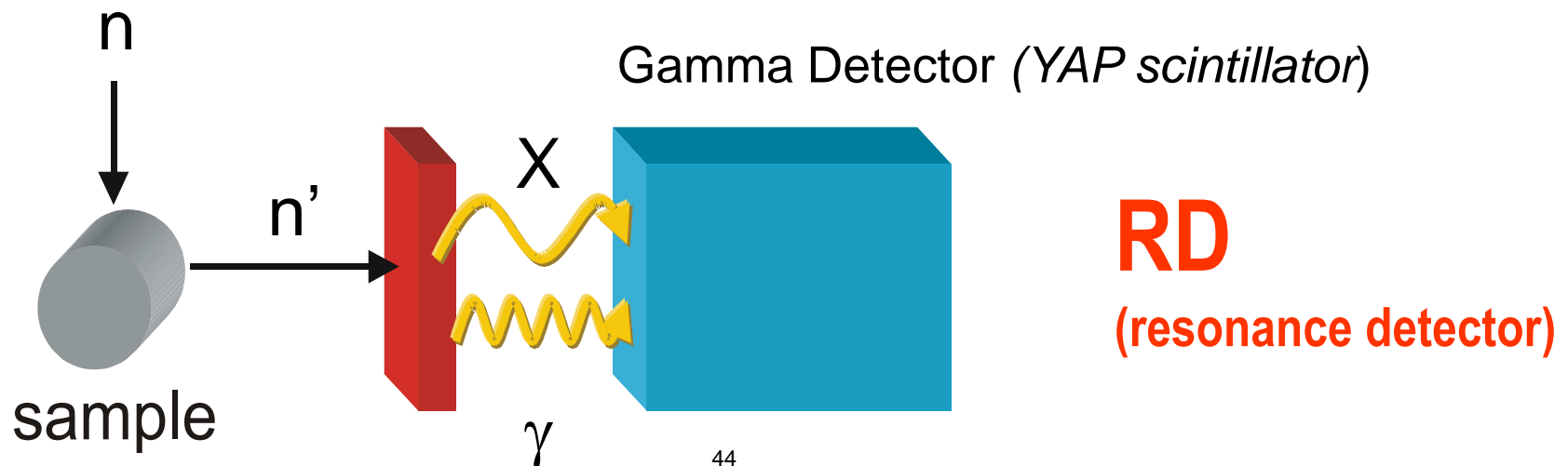
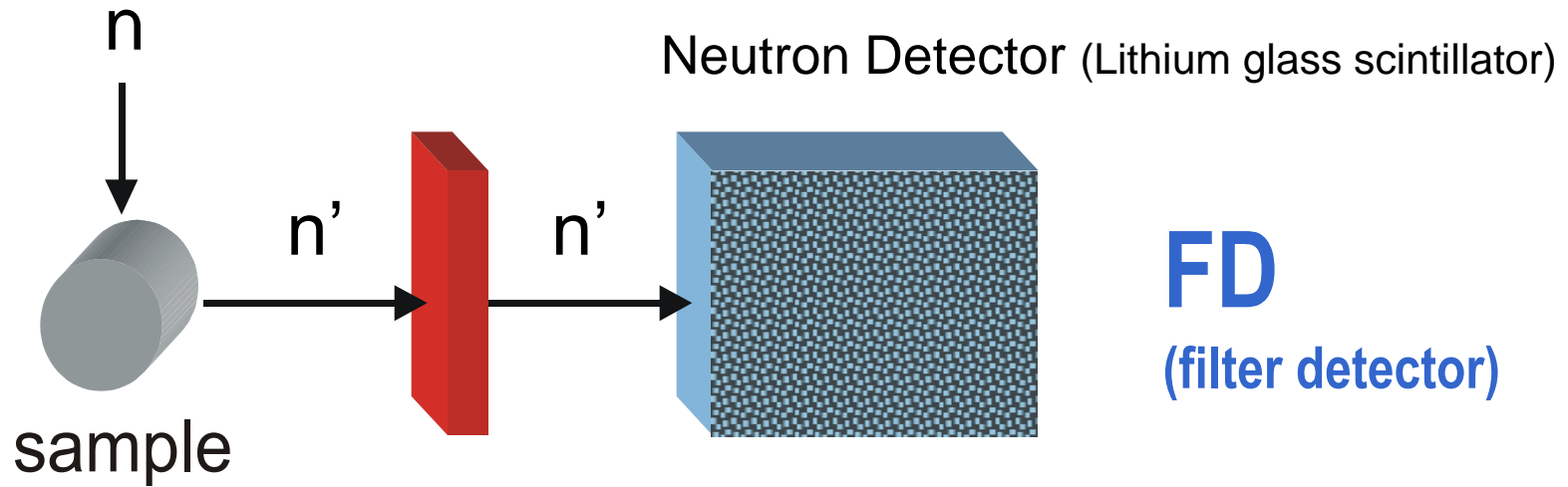
$$t = t_0 + \frac{L_0}{v_0} + \frac{L_1}{v_1}$$

Total Cross Section of Tantalum

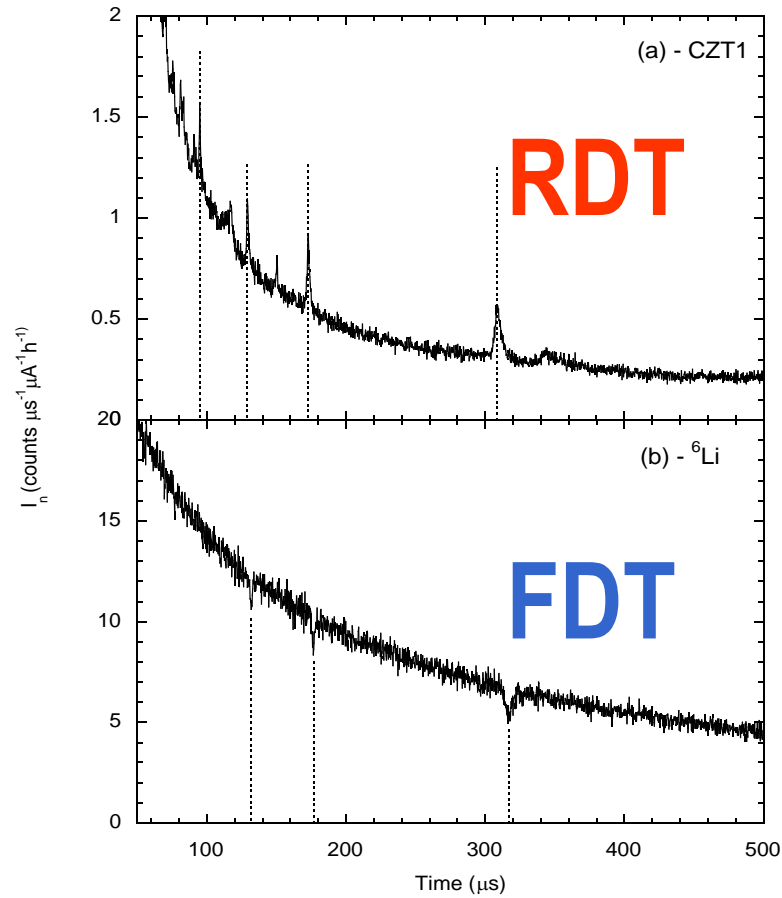
Tantalum is essentially
 monoisotopic ^{181}Ta and is
 used as a neutron converter
 sensitive to energies near
 4.28 eV.



Neutron detection techniques for epithermal neutrons



TOF spectra for FD (neutron detector) and RD (γ detector)



Pb sample
U foil

Resonance Detector principles

Two step process

- i) Neutron absorption and conversion through **(n, γ) reaction**
- ii) **Detection** of the emitted prompt gammas

RD properties

- The absorbing resonance fixes the final neutron energy
- Neutron conversion controls mainly the **energy resolution ($\Delta E/E$)**
- Ability to detect gammas controls the **signal to background ratio (S/B)**

Advantages over Li-glass detectors

- no principle need for background subtraction
- no $1/v$ decrease of the detection efficiency:
 - i) detection efficiency not dependent on the neutron energy
 - ii) high efficiency for epithermal neutrons (10-100 eV)

Choice of the resonant element

Neutron absorbing resonance

$$\sigma(E) = \frac{\sigma_0}{1 + 4(E - E_0)^2 / \Gamma^2}$$

(Breit Wigner)

E_0 neutron resonance energy

σ_0 peak cross section (at $E=E_0$)

Γ (FWHM) intrinsic resonance width

Criteria for resonant elements

- Resonance energy: **$E_0=10-100$ eV**
- Isolated resonance (to avoid overlapping with other resonances)
- High cross section (high conversion efficiency) \Rightarrow **$\sigma_0 = 10^4-10^5$ b**

- Narrow resonance (low $\Delta E/E$)

$\Rightarrow \Gamma \sim 100 \text{ meV}$

$\Rightarrow \Delta \sim 100 \text{ meV}$ (Thermal Doppler broadening)

- Foil thickness

Compromise between neutron absorption probability, $P(E_n)$, and $\Delta E/E$

$$P(E_n) = 1 - \exp(-N_d \cdot \sigma)$$

$$N_d = \rho \cdot t$$

$\Rightarrow N_d \cdot \sigma_0 = 1$

- High yield of low energy gammas (10-300 keV) \Rightarrow choice of suitable detector

Other desirable features: *high isotopic abundance, exist as metallic or oxide, low gamma self-absorption*

Best Isotopes

	i.a. (%)	density (g/cm ³)	E ₀ (eV)	σ ₀ (barn)	Γ (meV)	Δ (T=295 K) (meV)	Δ (T=75 K) (meV)
¹³⁹ La ₅₇	99.9	6.1	72.2	5969	96.0	231	125
¹⁵⁰ Sm ₆₂	7.4	7.4	20.7	56207	109.0	119	66
²³⁸ U ₉₂	99.3	18.9	6.7	23564	25.0	54	31
	“	“	20.9	37966	34.0	96	55
	“	“	36.7	42228	57.0	127	73
	“	“	66.0	20134	48.0	170	98

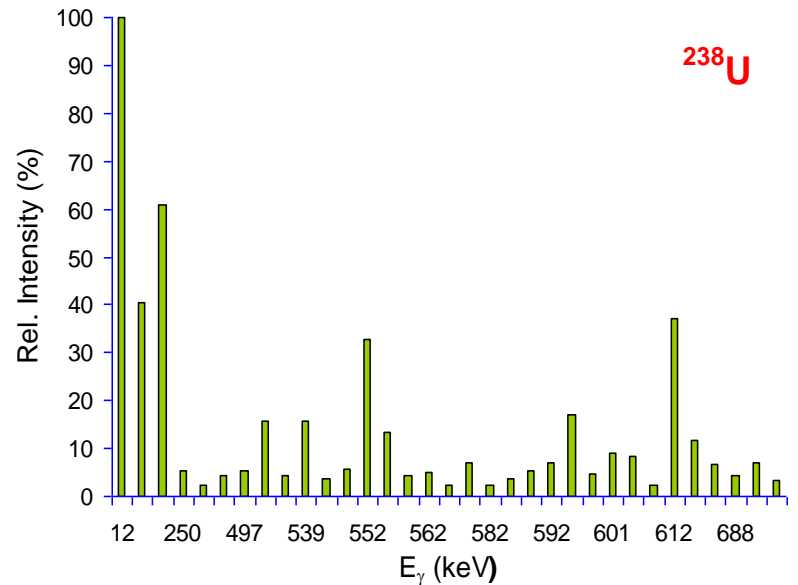
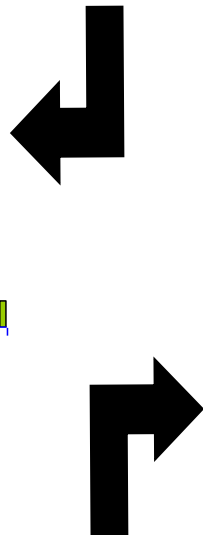
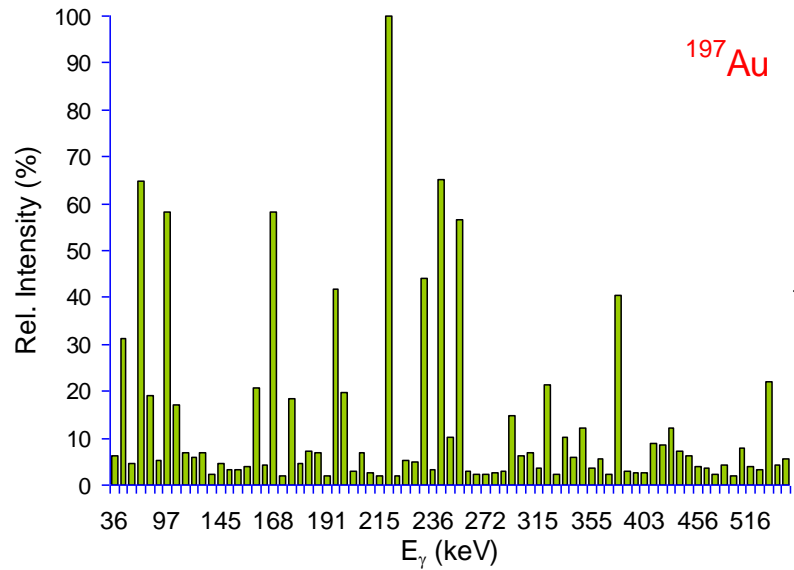
Gamma yield (absolute) exists for thermal neutron capture, but incomplete database for resonant neutron capture

¹³⁹ La ₅₇	218 keV	9 %	²³⁸ U ₉₂	12 keV
	32 %			
	288 keV	9 %		48 keV
	13 %			
				60 keV
	12 %			

Suitable isotopes for eV neutron energy selection

	% isot.	Z	A	densita' g/cm ³	N atom/cm ³	Eris eV	σ_0 barn	$\sigma_{\text{eff a 295K}}$ barn	λ_n μm	$d^*5^*\lambda_n$ g	$\sigma_{\text{eff a 75K}}$ barn
In	4,3	49	113	7,3	3,9E+22	14,6	9965	3837	66,9	1,223	5791
La	99,9	57	139	6,1	2,7E+22	72,2	5969	1762	213,2	3,275	2769
Sm	7,4	62	150	7,4	3,0E+22	20,7	56207	29108	11,6	0,214	39486
Gd	20,6	64	156	7,9	3,0E+22	33,2	11078	4854	67,5	1,334	6811
Dy	2,3	66	160	8,5	3,2E+22	10,5	19229	12179	25,5	0,545	15214
	2,3	66	160	8,5	3,2E+22	20,5	16165	9188	33,9	0,723	11923
Er	27,1	68	168	8,5	3,1E+22	79,7	11203	4096	79,8	1,703	5993
	14,9	68	170	8,5	3,0E+22	95,0	26393	23711	13,9	0,298	25396
Hf	0,2	72	174	13,3	4,6E+22	70,0					
	5,2	72	176	13,3	4,5E+22	48,0	36842	21132	10,4	0,346	26852
	5,2	72	176	13,3	4,5E+22	68,0					
	27,1	72	178	13,3	4,5E+22	7,8	153848	107369	2,1	0,069	127948
	35,2	72	180	13,3	4,4E+22	72,6	16838	6136	36,7	1,218	8657
W	26,3	74	182	19,3	6,4E+22	4,2	18828	10209	15,3	0,740	12354
	26,3	74	182	19,3	6,4E+22	21,1	46877	24395	6,4	0,310	29749
	26,3	74	182	19,3	6,4E+22	115,0					
Os	1,6	76	187	22,6	7,3E+22	12,7	16672	9563	14,4	0,812	11063
	26,4	76	190	22,6	7,2E+22	91,6	6777	2121	65,9	3,719	2625
U	100,0	92	238	18,9	4,8E+22	6,7	23564	7570	27,6	1,305	11250
U	100,0	92	238	18,9	4,8E+22	20,9	37966	9864	21,2	1,002	15119
U	100,0	92	238	18,9	4,8E+22	36,7	42228	13363	15,6	0,739	19913
U	100,0	92	238	18,9	4,8E+22	66,0	20134	4357	48,0	2,268	6813

Energy and relative intensities of γ -rays



Suitable γ detectors for the RDS

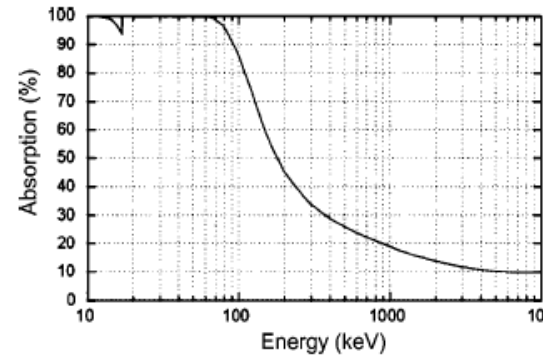
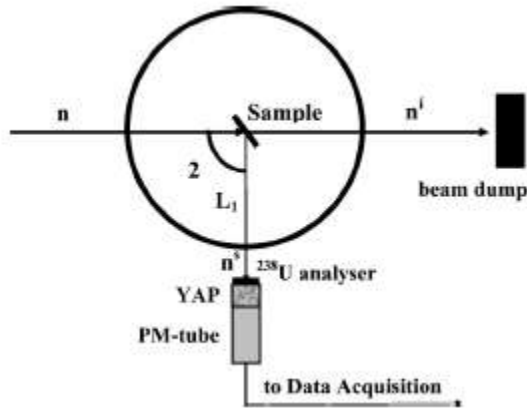
Scintillators

- 1) NaI(Tl): good efficiency and energy resolution for MeV gamma ray. High sensitivity to neutron background (need of shielding).
- 2) **YAP**: good efficiency and moderate energy resolution. Low sensitivity to neutron background

Solid State

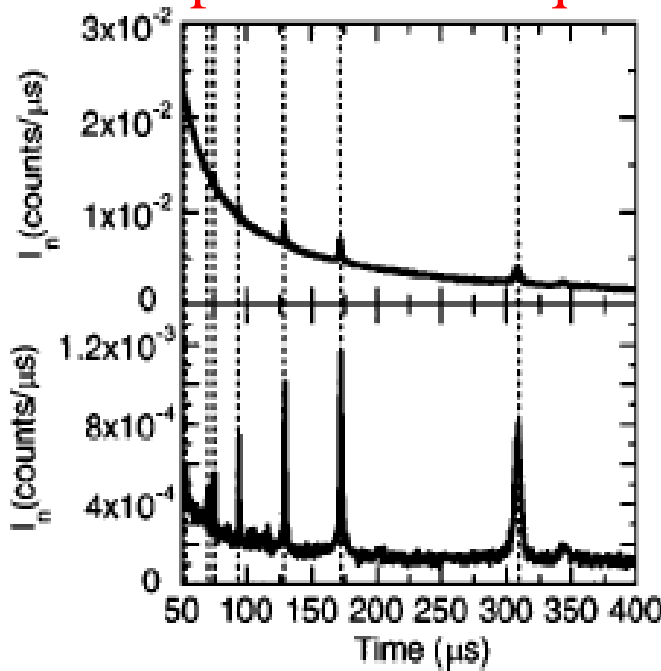
- 1) HpGe: excellent energy resolution, adequate efficiency. Radiation damage. Need to operate at cold temperature (77K)
- 2) Silicon: good for x-ray and low energy γ ray. Requires some cooling. Radiation damage
- 3) **CdZnTe** (CZT): Good efficiency and high energy resolution. Operate at room temperature. small areas.

YAP detector



6mm thick

Biparametric acquisition



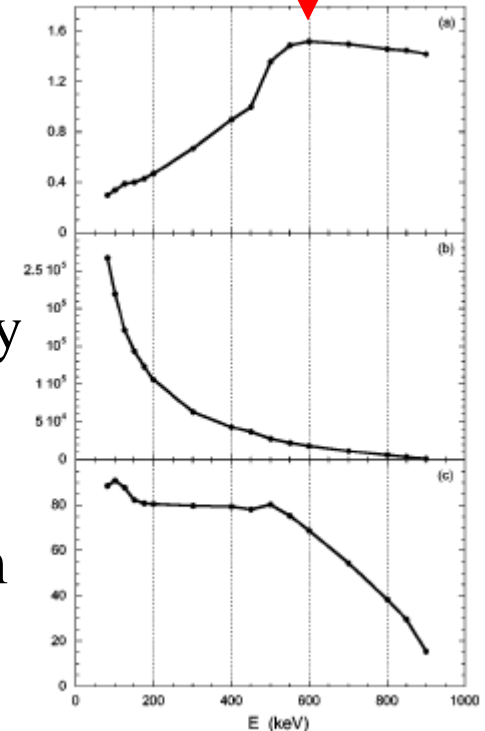
>40keV

>600keV

S/B

Intensity

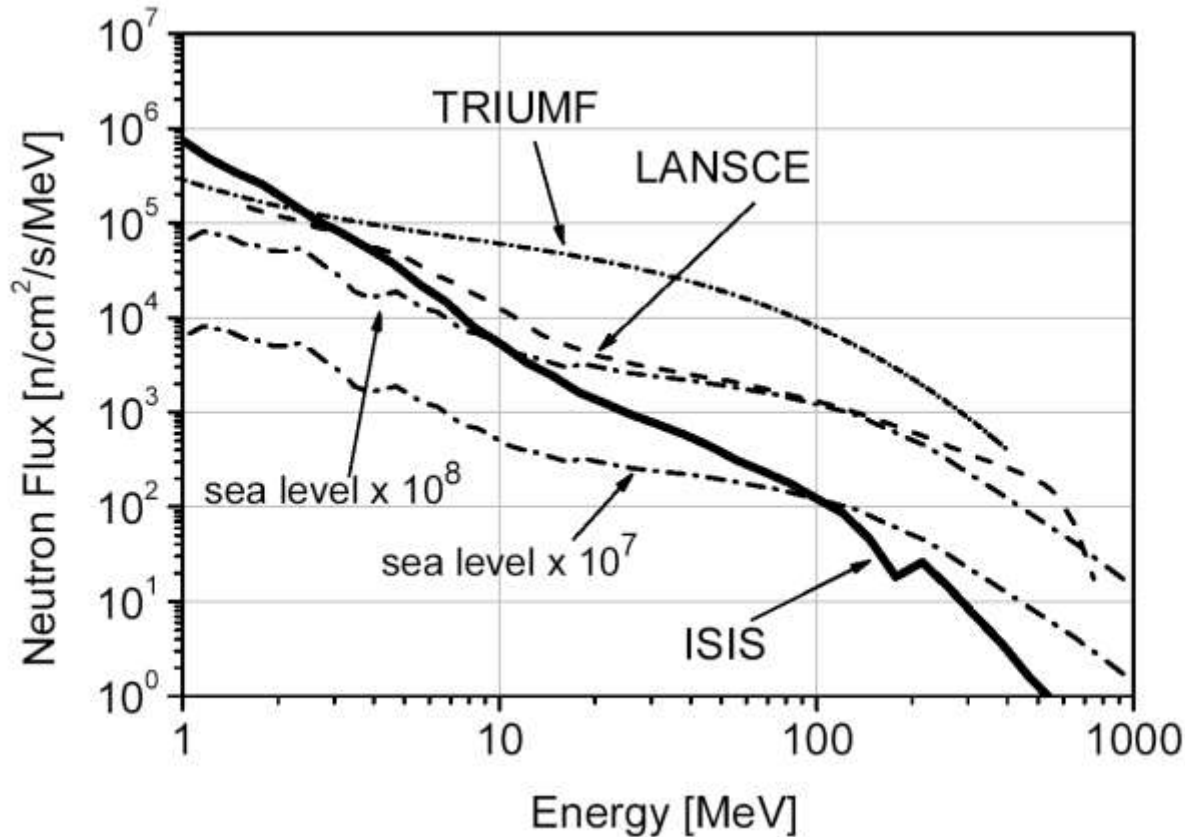
fom



Fast neutrons detection

- Spherical dosimeters
- Scintillators
- ^3He proportional counters
- Proton Recoil Telescope
- Activation threshold targets
- Bonner Sphere
- TFBC
- Diamond detectors

Fast neutron flux on VESUVIO (at ISIS)

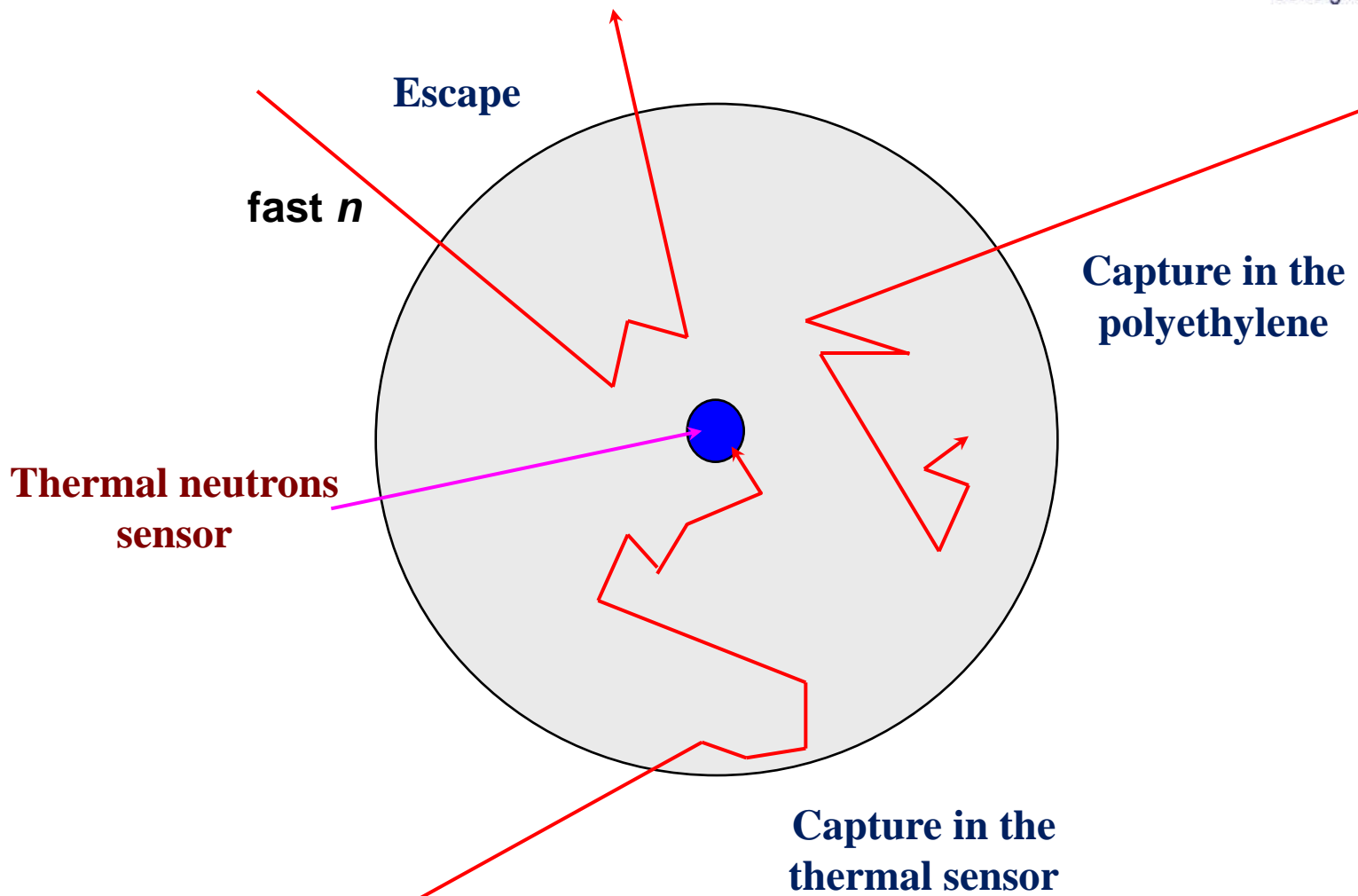


Measured with
 activation
 targets

Enormous energy range 1-800 MeV!



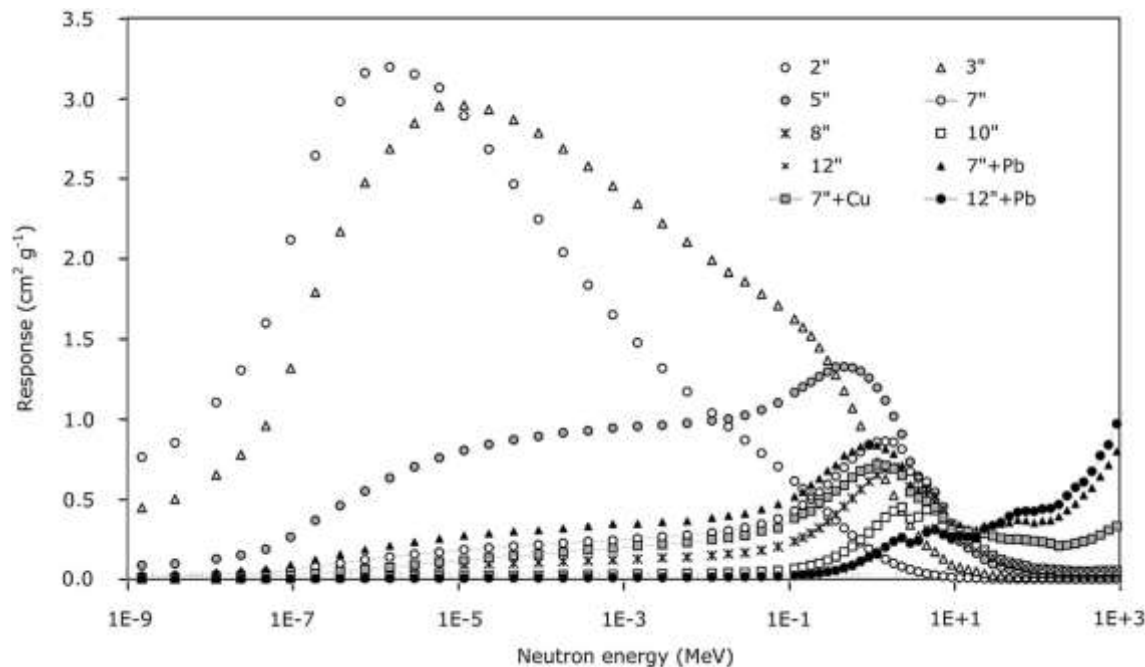
Principle of operation



From the measured activity on the sensor after a period of irradiation the neutron flux at the selected energy range is found

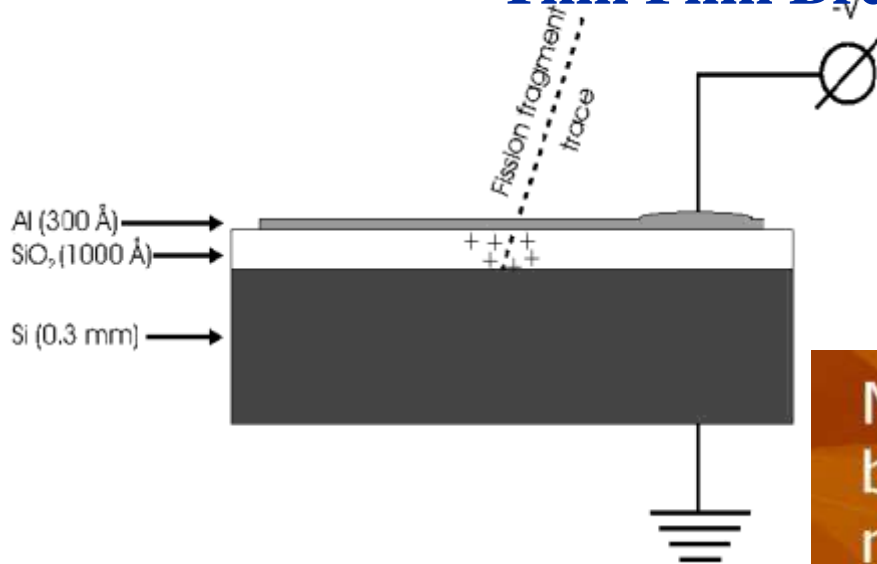
Modified Bonner Spheres by including metal inserts to allow for $n(x,n)$ reactions to occur





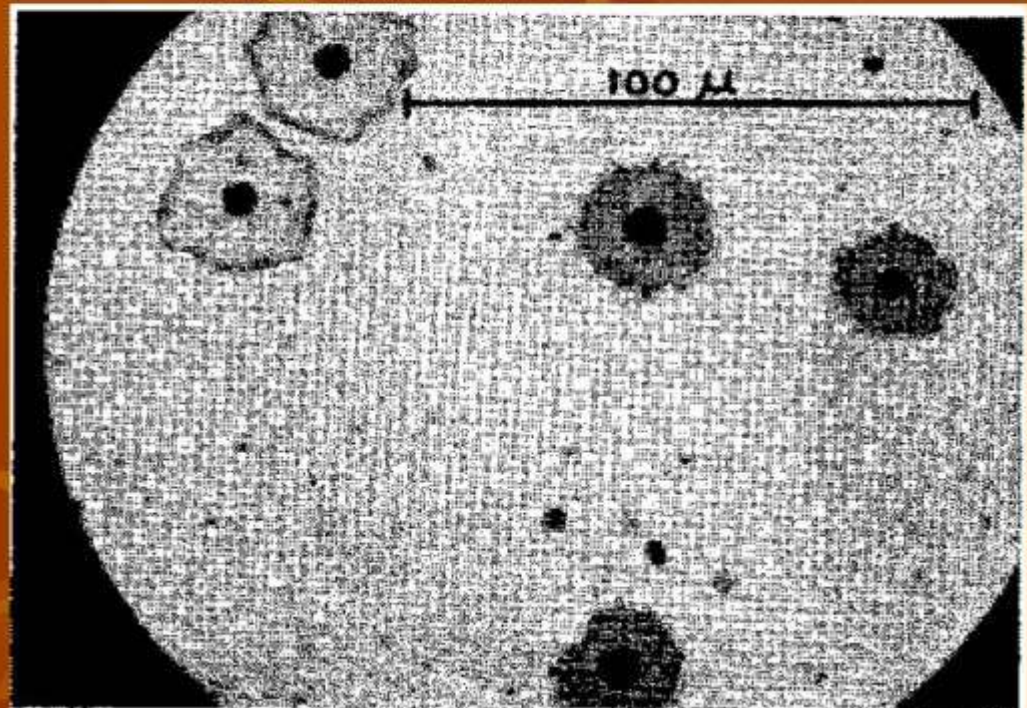
The very broad response function means that complicated deconvolution codes are needed to infer the incoming neutron spectrum from the measurement,

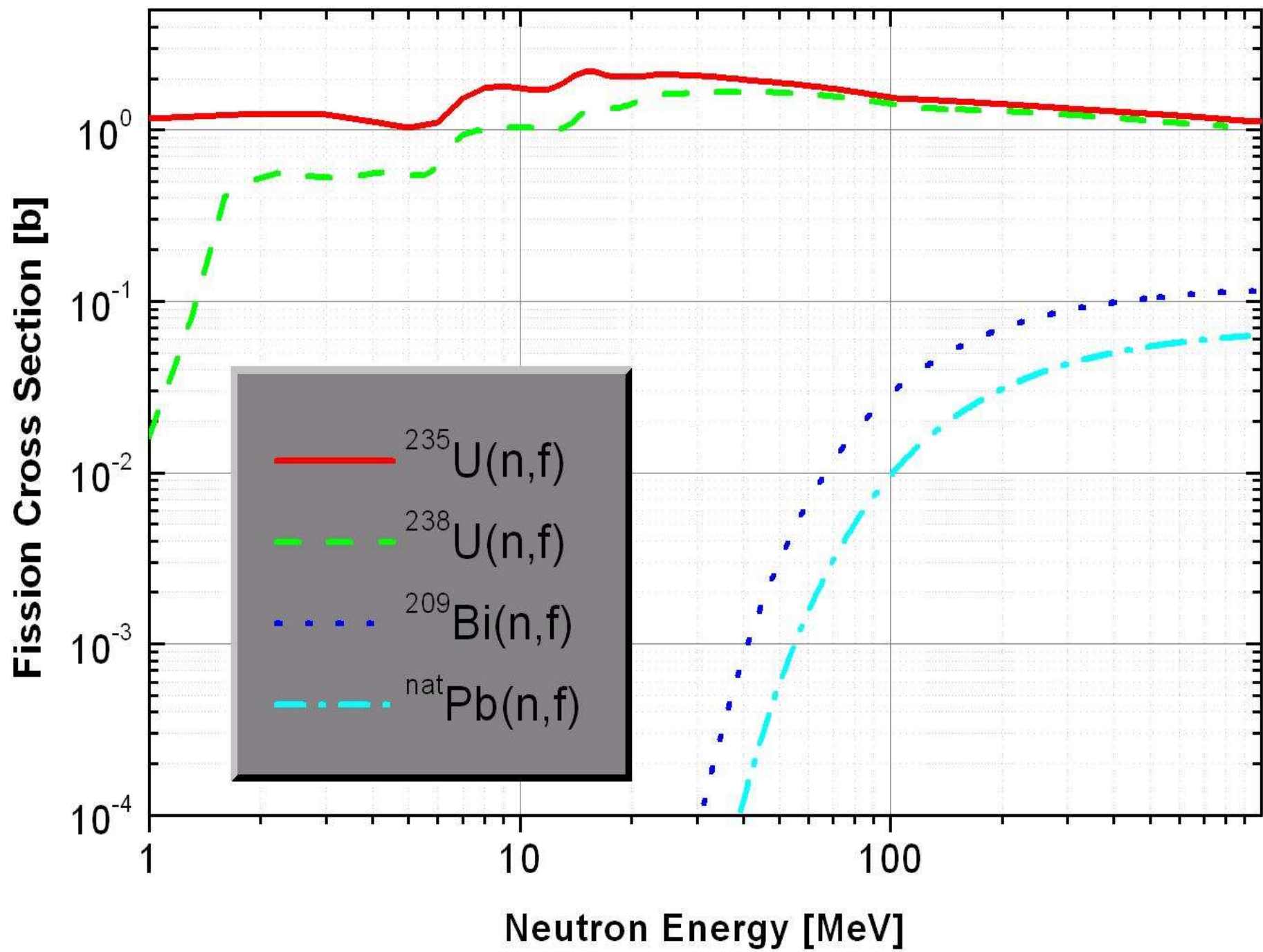
Thin Film Breakdown Counter



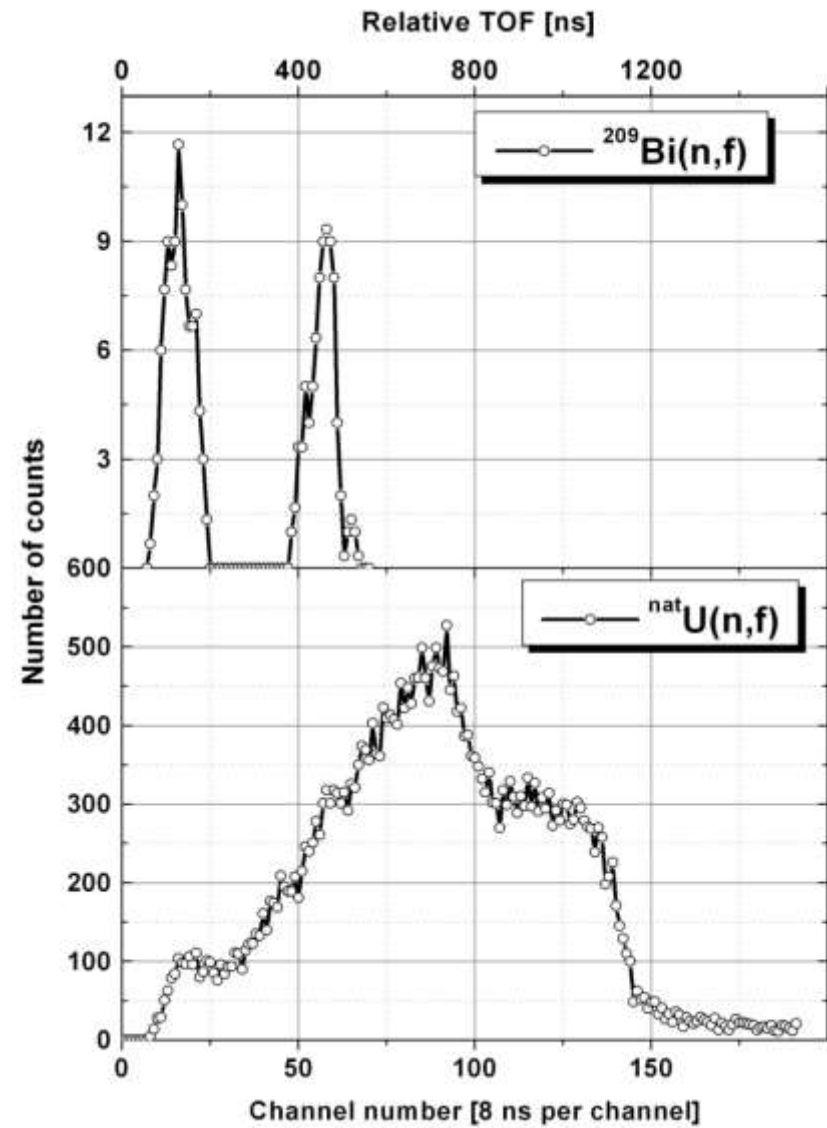
Schematic of a TFBC and the principle of its operation: an incident fission fragment produces an electrical breakdown in the SiO₂ layer.

Micro-photographs of electrical breakdowns in MOS-capacitor made in reflect light



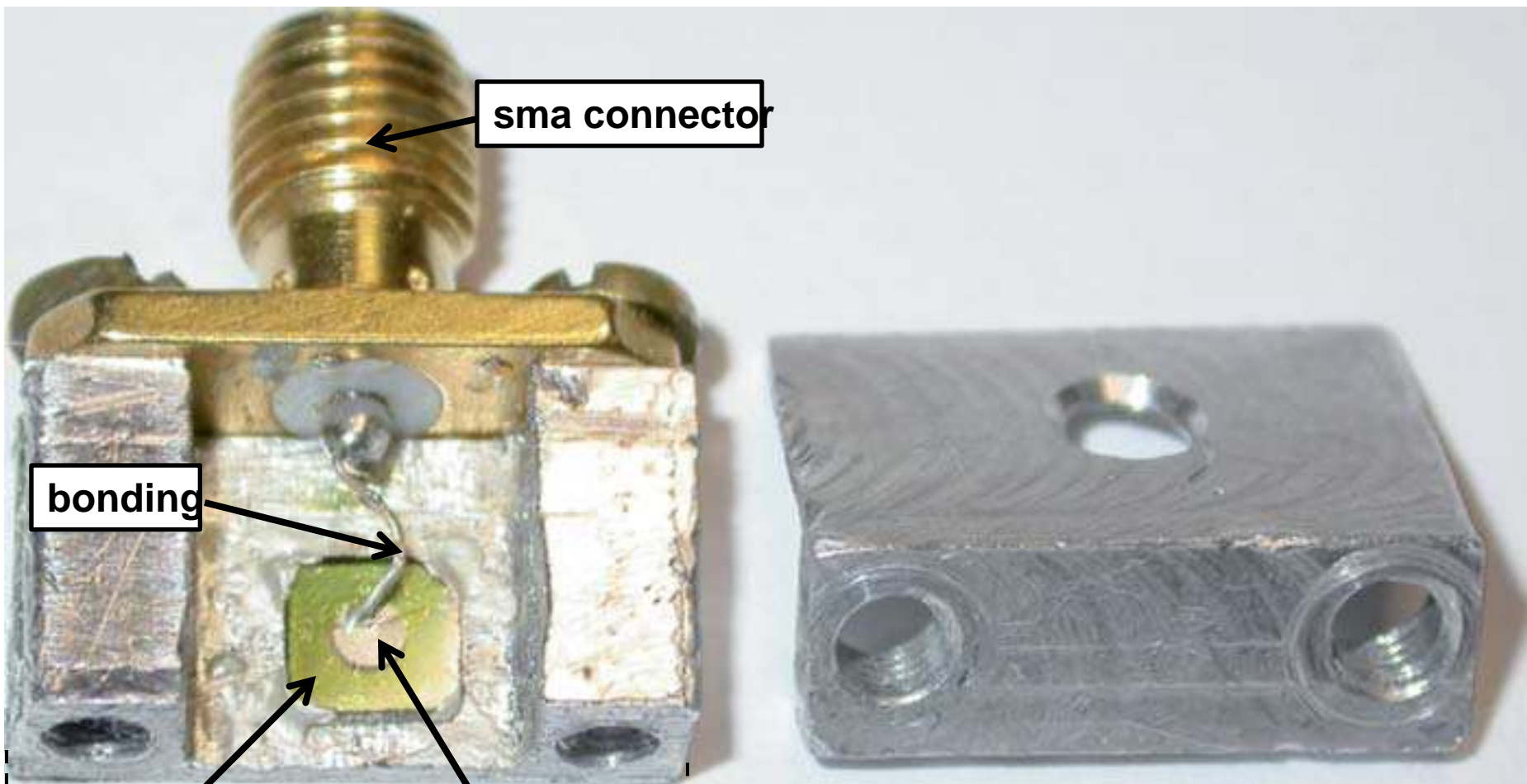


Picture of a TFBC array



Neutron ToF spectra

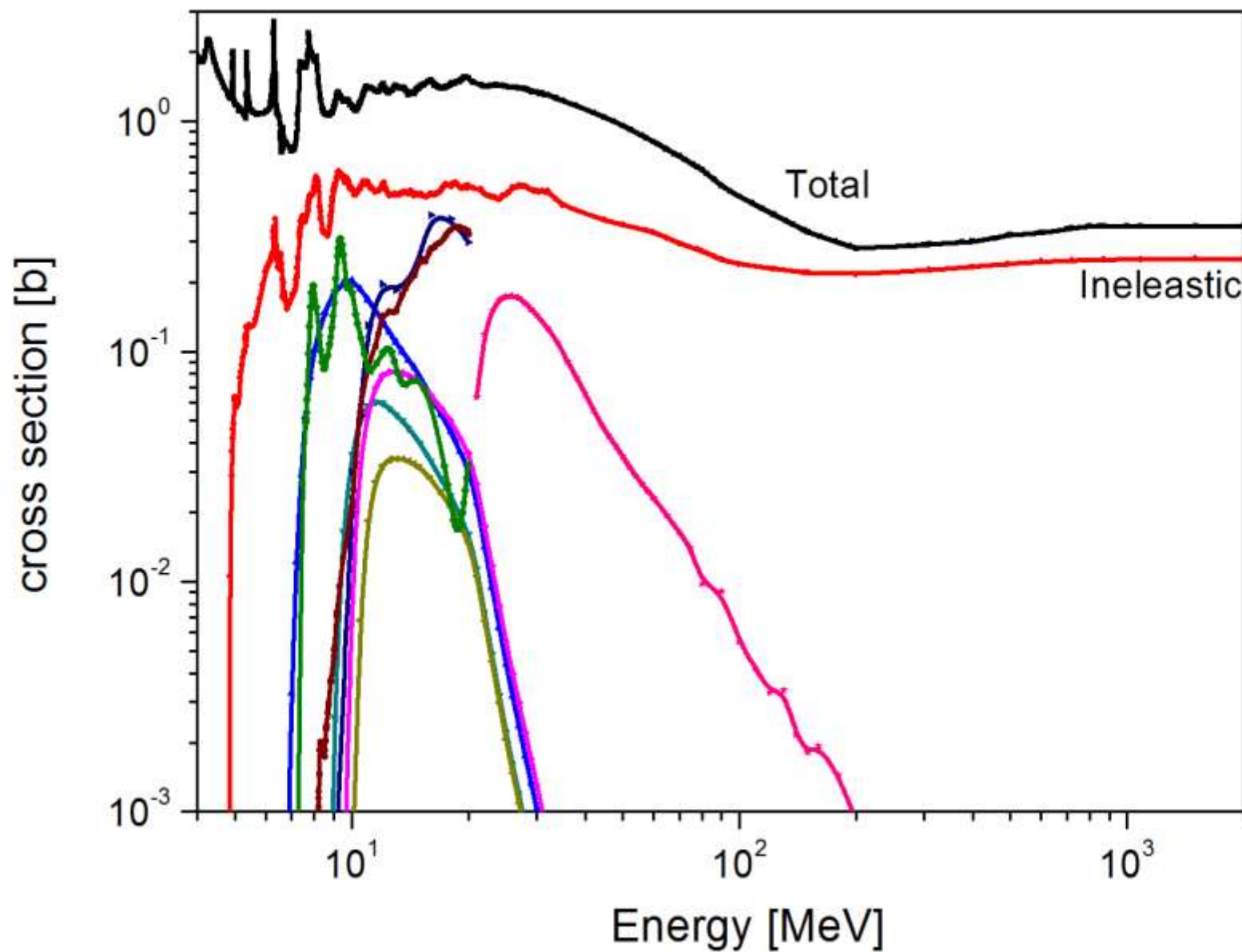
Diamond detector grown by Chemical Vapor Deposition



CVD diamond **Al contact**

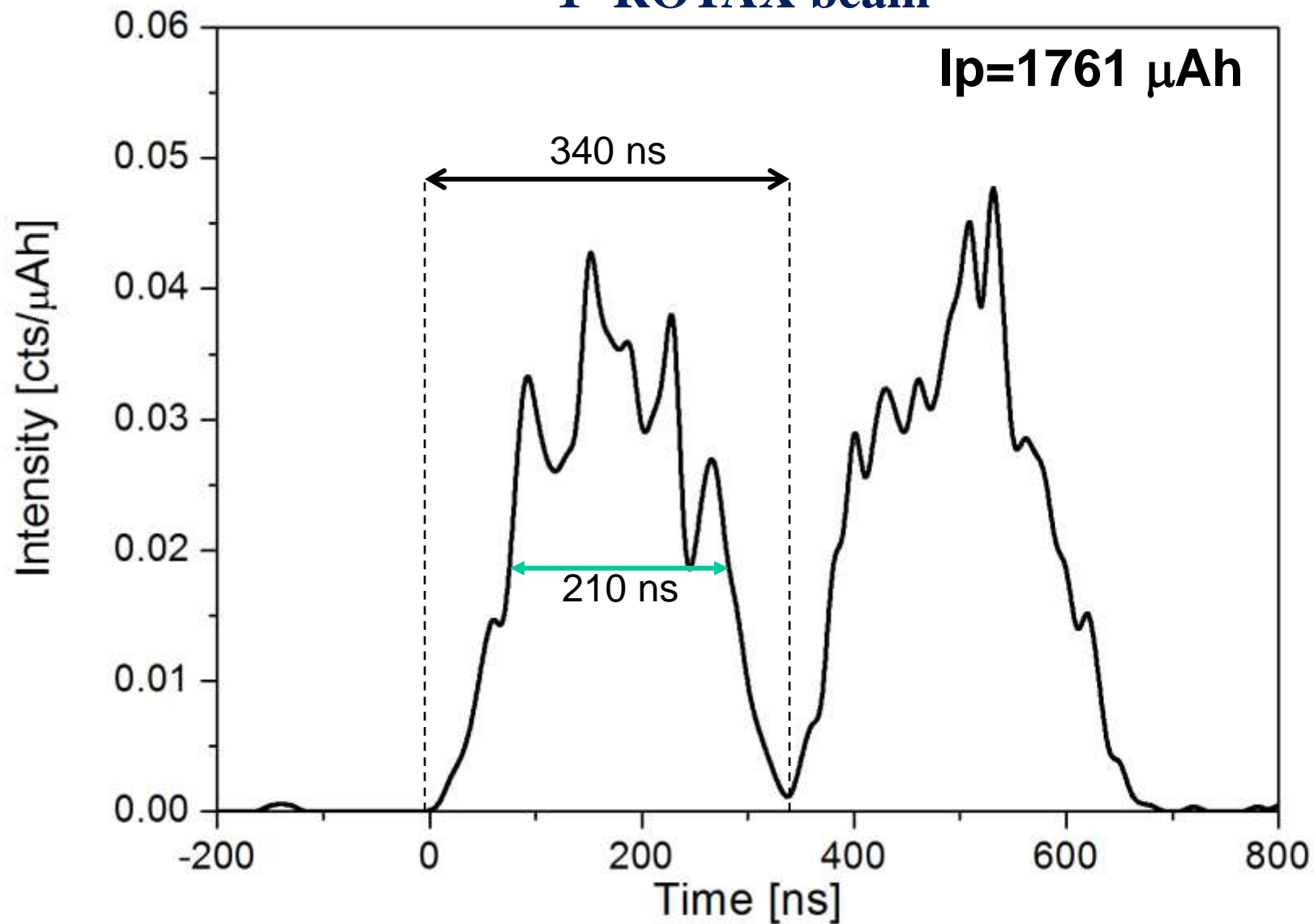
Marco Tardocchi 26.09.2010

n - ^{12}C neutron cross sections



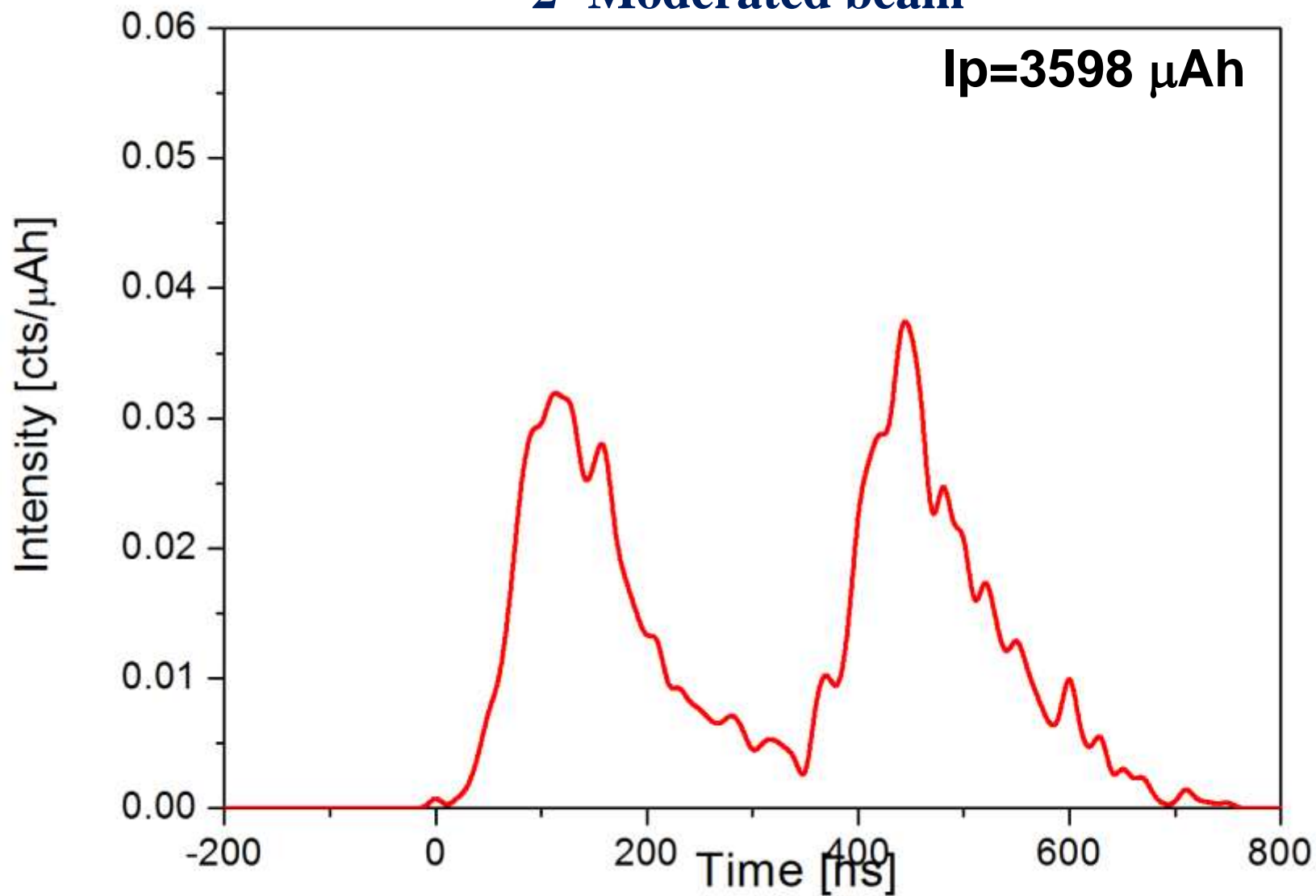
TOF SPECTRUM FROM DIAMOND

1- ROTAX beam

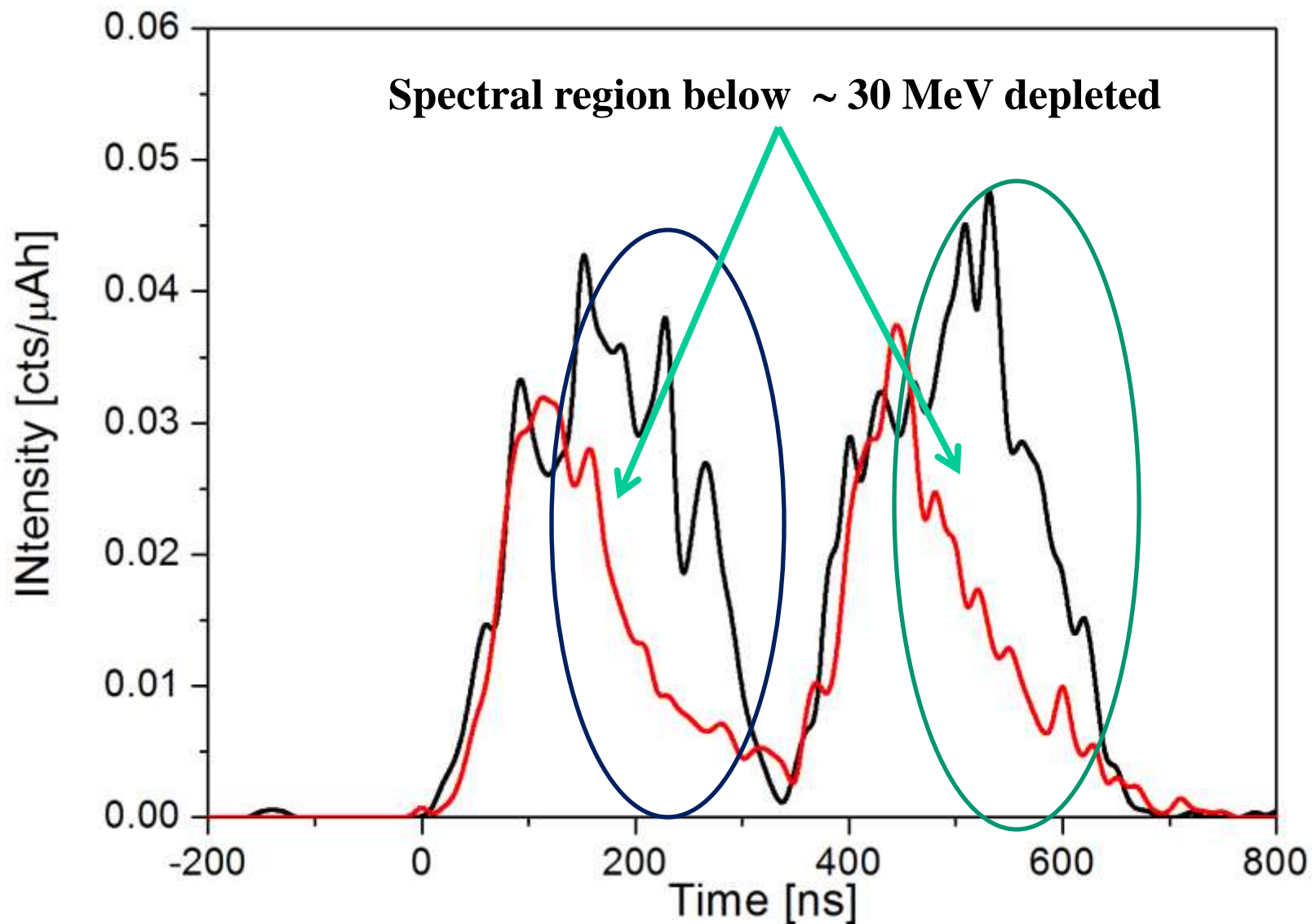


TOF SPECTRUM FROM DIAMOND

2- Moderated beam



TOF SPECTRA FROM DIAMOND

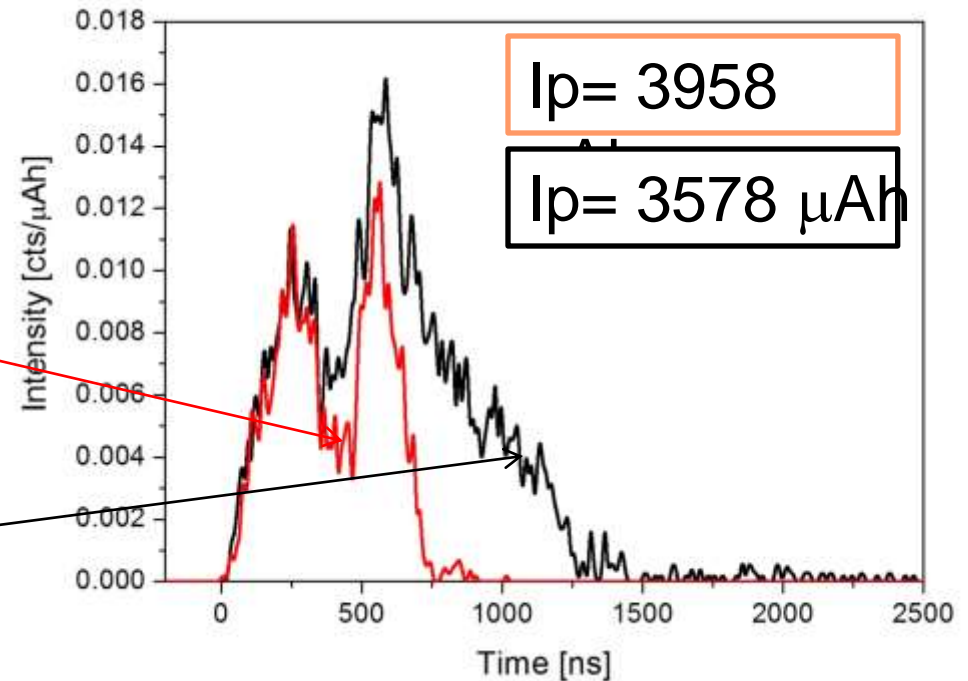


Modifying the diamond response:

1- with a fissile material

Only diamond (25 μm)

Diamond + ^{235}U sheet 30 μm



END

Spherical dosimeters

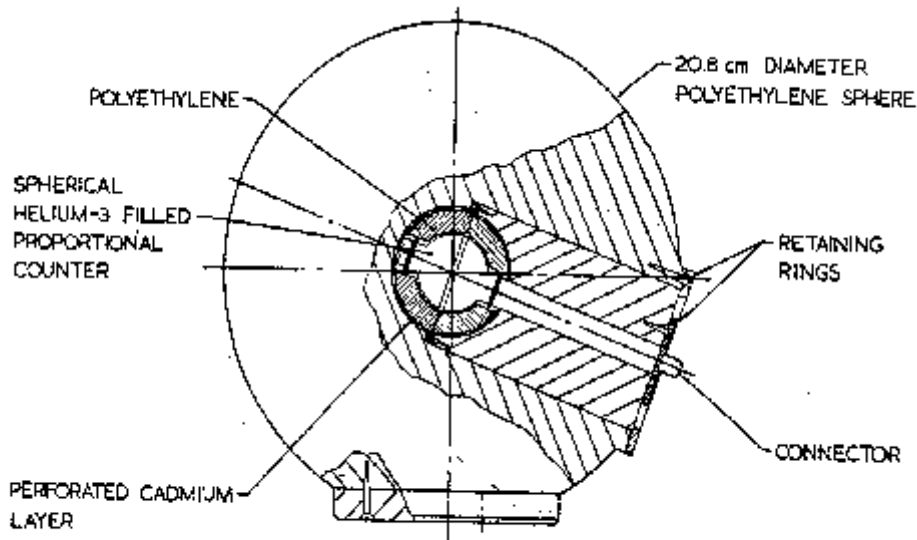


Figure 15.5 A spherical neutron dosimeter based on a ^3He neutron detector. (From Leake.¹⁴)

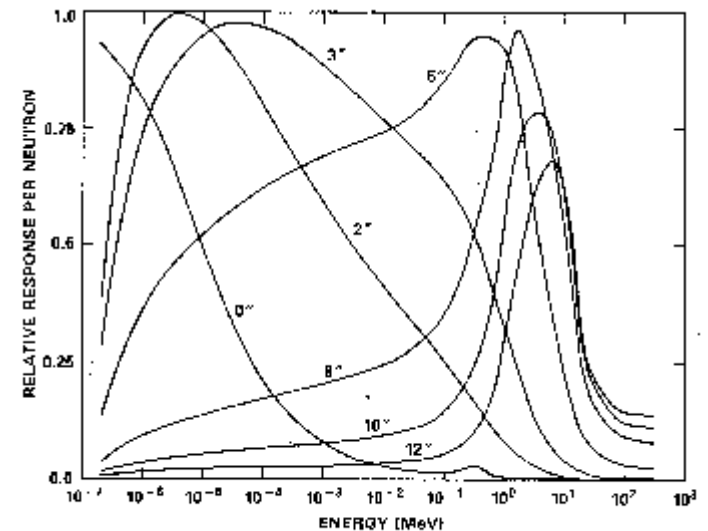
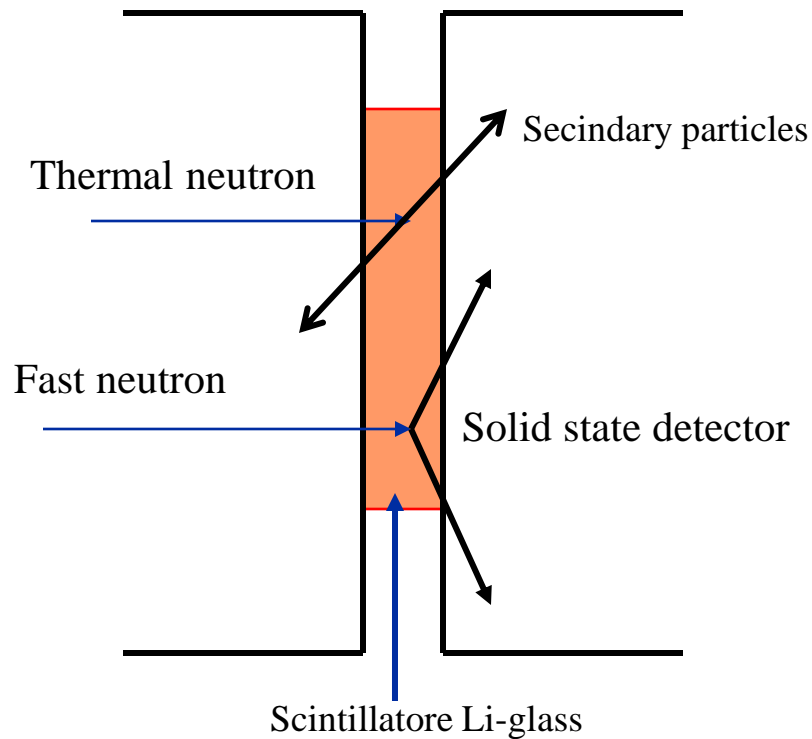


Figure 15.2 The energy dependence of the relative detection efficiencies of Bonner sphere neutron detectors of various diameters up to 12 inches. (From Johnson et al.²)

^6Li -glass scintillators



The use of coincidence produces
a lowering in the efficiency with
increasing neutron energy
($E_n \geq Q$ -value of the reaction)

Some characteristics

	NE902	NE905	NE908	NE912
D (gr/cm ³)	2.6	2.48	2.674	2.55
<i>n</i>	1.58	1.55	1.57	1.55
T_{fusione} (°C)	1200	1200	1200	1200
λ_{max} (nm)	395	395	395	397
Light emission (rel.antracene)	22-34%	20-30%	20%	25%
Decay time (ns)	75	100	75	75
Arr. ⁶ Li	95%	95%	95%	95%
Activity α (/min)	100-200	100-200	100-200	10
$\Delta E/E$	13-22 %	15-28 %	20-30 %	20-30 %

^3He proportional counters

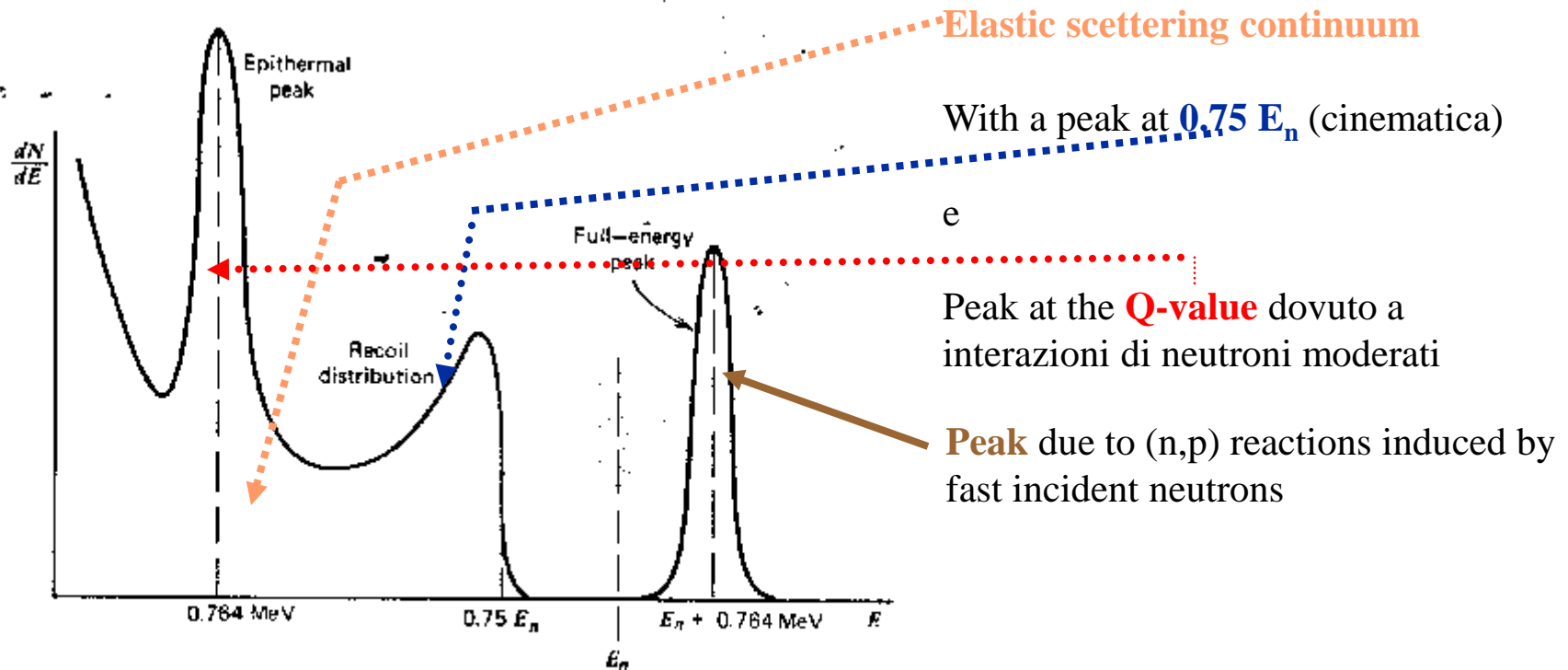
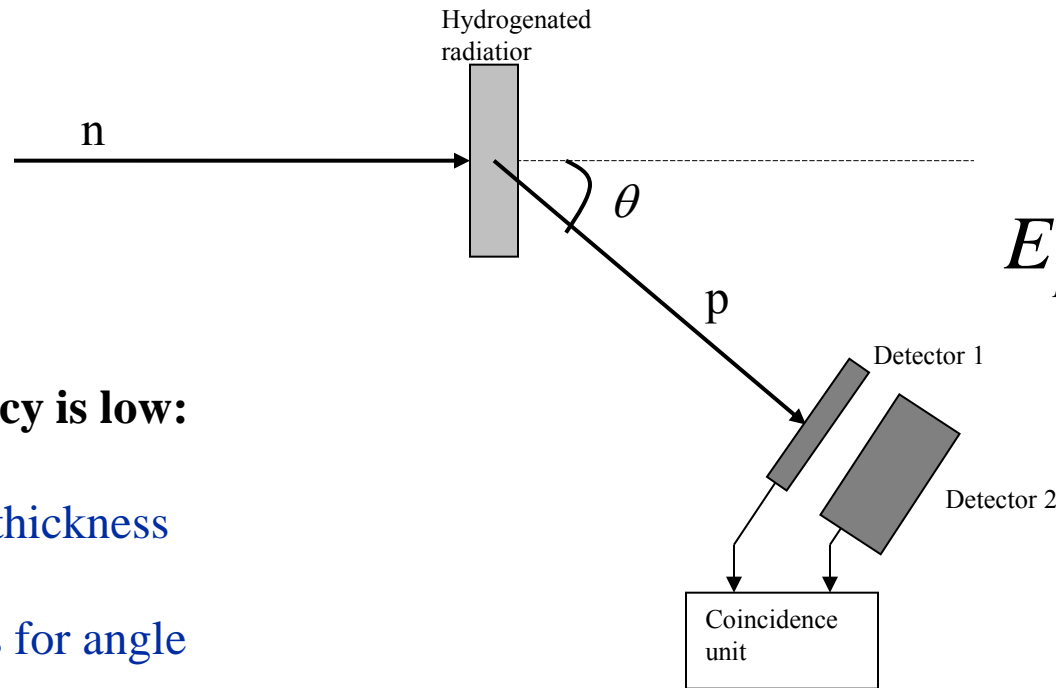


Figure 15.11 Differential energy spectrum of charged particles expected from fast neutrons incident on a ^3He detector.

Proton Recoil Telescope

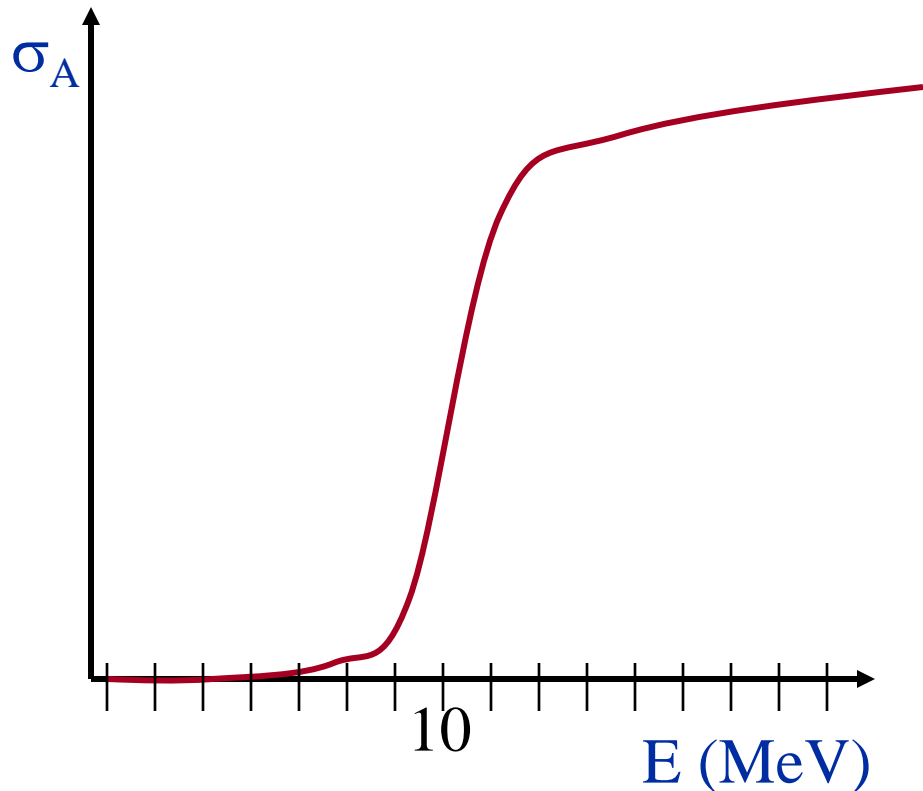


$$E_p = E_n \cos^2 \theta$$

Efficiency is low:

- small radiator thickness
- small detectors for angle determination

Activation threshold technique

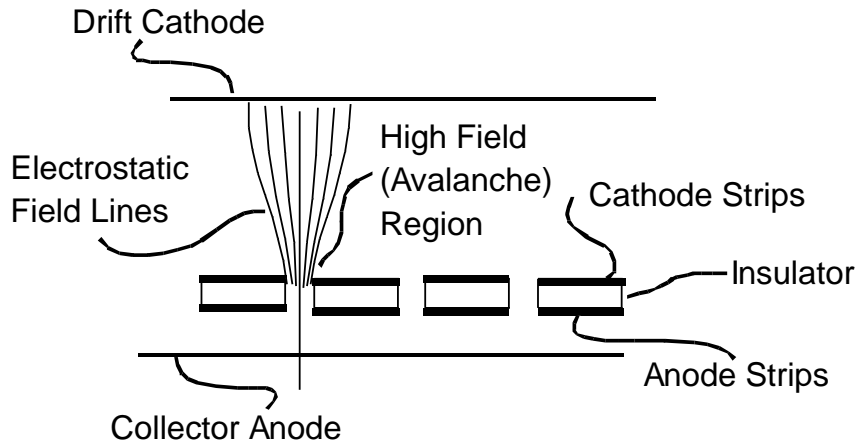


A target of a proper material is irradiated with a neutron beam and after an irradiation time Δt is removed from the beam and the induced activity is measured

Some examples

Material	Reaction	Ab.Is.(%)	H.L	E_γ	Threshold (MeV)
F	$^{19}\text{F}(n,2n)^{18}\text{F}$	100	109.7min	0.511	11.6
Mg	$^{24}\text{Mg}(n,p)^{24}\text{Na}$	78.7	15.0 h	1.368	6.0
Al	$^{27}\text{Al}(n,\alpha)^{24}\text{Na}$	100	15.0 h	1.368	4.9
Fe	$^{56}\text{Fe}(n,p)^{56}\text{Mn}$	91.7	2.56 h	0.84	4.9
Co	$^{59}\text{Co}(n,\alpha)^{56}\text{Mn}$	100	2.56 h	0.84	5.2
Ni	$^{58}\text{Ni}(n,2n)^{57}\text{Ni}$	67.9	36.0 h	1.37	13.0
Cu	$^{65}\text{Cu}(n,2n)^{64}\text{Cu}$	69.1	9.8 min	0.511	11.9
Zn	$^{64}\text{Zn}(n,p)^{64}\text{Cu}$	48.8	12.7 h	0.511	2.0
In	$^{115}\text{In}(n,n')^{126}\text{In}$	95.7	4.5 h	0.335	0.5
I	$^{127}\text{I}(n,2n)^{126}\text{I}$	100	13.0 d	0.667	9.3

Micro-Strip Gas Counter



Electrodes printed lithographically, producing small features. Implies

- High spatial resolution.
- High field gradients.
- Charge localization.
- Fast recovery.

